UNIVERSIDAD COMPLUTENSE DE MADRID

FACULTAD DE MEDICINA
Departamento de Radiología y Medicina Física

TESIS DOCTORAL

Estudio las alteraciones hemodinámicas en fases tempranas de la enfermedad de Alzheimer mediante imagen por resonancia magnética multimodal: estructural, perfusión y difusión

MEMORIA PARA OPTAR AL GRADO DE DOCTOR

PRESENTADA POR

María La Calle Aurioles

Directores

Manuel Desco Menéndez
María Luisa Vega González

Madrid, 2014

UNIVERSIDAD COMPLUTENSE DE MADRID

FACULTAD DE MEDICINA

Departamento de Radiología y Medicina Física

Tesis Doctoral

ESTUDIO DE LAS ALTERACIONES HEMODINÁMICAS EN FASES TEMPRANAS DE LA ENFERMEDAD DE ALZHEIMER MEDIANTE IMAGEN POR RESONANCIA MAGNÉTICA MULTIMODAL: ESTRUCTURAL, PERFUSIÓN Y DIFUSIÓN.

Autora

MARÍA LA CALLE AURIOLES

Directores de Tesis

MANUEL DESCO MENÉNDEZ

Doctor en Medicina e Ingeniero de Telecomunicación

MARÍA LUISA VEGA GONZÁLEZ

Doctora en Medicina

MADRID, 2014

A Santiago Reig y mi hermano Leo

AGRADECIMIENTOS:

Este proyecto de tesis doctoral se enmarca dentro de un proyecto FIS (PI052271) del Instituto de Salud Carlos III, Ministerio de Economía y Competitividad. La financiación recibida por el autor de esta tesis procede de una Ayuda Predoctoral de Formación en Investigación en Salud (PFIS) (FI08/00585) del Instituto de Salud Carlos III, Ministerio de Economía y Competitividad y de una beca de investigación del departamento de Bioingeniería e Ingeniería Aeroespacial de la Universidad Carlos III de Madrid.

Este trabajo no habría sido posible sin el apoyo de mis compañeros del Laboratorio de Imagen Médica del Hospital General Universitario Gregorio Marañón, especialmente de Yasser Alemán, Javier Navas y José María Mateos. También han sido de gran ayuda mis reuniones con Juan Guzmán de Villoria, de la Unidad de Radiología, y con Javier Olazarán e Isabel Cruz, de la Unidad de Neurología.

Agradecer también a Manuel Desco su confianza en mí para realizar este trabajo y su tiempo para revisar el manuscrito de tesis y los diversos artículos que han salido y saldrán a partir de este proyecto.

También me gustaría agradecer la generosidad y la valentía de todos los pacientes y voluntarios sanos que han participado en este estudio. Gracias por aportar vuestro granito de arena al inmenso mundo de la ciencia.

Por último, gracias a todos los familiares y amigos que han estado apoyándome en los momentos más difíciles y decisivos de esta etapa.

ÍNDICE

ABREVIATURAS EN CASTELLANO

EA Enfermedad de Alzheimer

DCL Deterioro cognitivo leve

LCR Líquido cefalorraquídeo

RM Resonancia magnética

SB Sustancia blanca

SG Sustancia gris

ABREVIATURAS EN INGLÉS

APP Amyloid precursor protein

CAA Cerebral amyloid angiopathy

CBF Cerebral blood flow

CBV Cerebral blood volume

CDR Clinical dementia rating

CT Computerized tomography

DTI Diffusion tensor imaging

DSC Dynamic Susceptibility Contrast

EPI Echo Planar Imaging

FA Fractional anisotropy

FOV Field of view

MD Mean diffusivity

MRI Magnetic resonance imaging

MTT Mean transit time

NFTs Neurofibrillary tangles

NPs Neuritic plaques

PET Positron emission tomography

PHFs Paired helical filaments

SPECT Single-photon emission computed tomography

SUMMARY

Introduction

Structural magnetic resonance imaging (MRI) and positron emission tomography (PET) are currently the most validated techniques for the in vivo diagnosis of Alzheimer's disease (AD). MRI technique also offers other less explored varieties of functional imaging which could become potential diagnostic tools in the future. This is the case of diffusion tensor imaging (DTI) that assesses the microstructural changes of white matter (WM) fibers, or perfusion MRI that provides information about cerebral microvasculature. Perfusion MRI has been proposed as a good alternative to nuclear medicine for the detection of cerebral hemodynamic changes in AD. However, due to the recent incorporation of the perfusion technique in the assessment of AD patients, there is no yet information in the literature about certain methodological aspects that could improve its diagnostic accuracy. Due to biological factors, brain perfusion presents a large physiological variability across subjects that make it difficult the detection of perfusion abnormalities in comparative analysis; this fact makes it necessary to perform an intensity normalization of perfusion images. When using nuclear medicine techniques, the cerebellum is the most commonly used reference region in perfusion studies in AD patients, since it has been reported to provide unbiased estimations. This knowledge has been directly extrapolated to perfusion studies with MRI, but no reports have evaluated the consequences of using different normalization regions in MRI studies, and the cerebellum has not yet been confirmed as an optimal reference region. On the other hand, there are no comparative studies on the sensitivity of different perfusion parameters (cerebral blood volume; CBV, cerebral blood flow; CBF) to the hemodynamic changes in the different stages of the disease. Since CBF seems to be more sensitive than CBV to functional changes in neurons, CBF may be purportedly more sensitive in the detection of the hemodynamic abnormalities in the earliest stages of the disease, therefore better detecting functional changes in asymptomatic patients than CBV. Finally, the combined study of MRI techniques (conventional, perfusion and diffusion) in the characterization of patients in early stages of AD could shed light on whether the hemodynamic changes observed in these patients have a direct relationship with brain atrophy or damage to the

neural connections. According to the so-called disconnection hypothesis, the loss of synaptic inputs from the medial temporal lobes may lead to a reduction in the activity of target neurons in allocortical areas and, consequently, to a decrease of CBF in those areas. The existence of a significant correlation between blood perfusion decrease in the cerebral cortex and microstructural changes in WM fibers that connect the hypoperfused areas with the medial temporal lobes could indicate damage in the physical links between these two regions functionally connected, thus providing an explanation to hemodynamic changes on the basis of a functional disconnection.

Objectives

The main objective of this thesis is to study methodological aspects of perfusion MRI to improve the detection of brain hemodynamic changes in early stages of AD, and to explore the relation of these hemodynamic changes with macro and microstructural changes that occur in the cerebral cortex and WM tracts respectively.

Specific objectives proposed in this thesis are the following:

• To find a reference region for intensity normalization of perfusion parametric maps to improve the detection of cerebral perfusion differences between patients in early stages of AD and controls in comparative studies.

• To evaluate which perfusion variable (CBV, CBF) is a better biomarker of the cerebral hemodynamic changes in the earliest stages of the disease.

• To find possible correlations between hemodynamic changes and cortical atrophy when the two pathological events coexist in the same cortical regions.

• To evaluate the "fractional anisotropy" (FA) parameter to assess possible changes in the microstructure of the WM tracts in patients.

• To measure the correlation between cortical atrophy in the medial temporal lobes and CBF decrease in the parietotemporal and frontal cortices.

• To measure the correlation between CBF decrease in the parietotemporal and frontal cortices and fractional anisotropy decrease in WM tracts connecting these cortical regions with the medial temporal lobes.

• To measure the correlation between cortical atrophy in the medial temporal lobes and fractional anisotropy decrease in WM tracts of the limbic system.

Material and Methods

A total of 74 subjects were recruited. Patients with cognitive impairment were prospectively recruited during routine clinical practice in the behavioural neurology clinic of the Hospital General Universitario Gregorio Marañón at the stage of mild cognitive impairment (MCI, n=37) or mild Alzheimer disease (AD=15). Control subjects (n=22) were chosen from volunteers attending the behavioral neurology clinic as patient caregivers and from among researchers' acquaintances. After two years of clinical follow-up patients were reclassified into three groups according to their final diagnoses: MCI group (n=17), MCI converters to dementia due to AD (MCI-c, n=16) and mild AD dementia (n=14). MRI-based structural, perfusion and diffusion data were obtained from all participants, although some perfusion and diffusion studies were excluded due to patient movement during the image acquisition. The software package FreeSurfer version 4.5.1 was used to obtain the gray matter (GM) volume and mean cortical thickness per region of interest (ROI). Giral-based ROIs were defined according to the Desikan-Killiany atlas. Whole-brain WM, GM volume of the bilateral hippocampi and amygdalae, and cerebellum were also segmented. Perfusion parametric maps were co-registered with the T1-weighted images using mutual information methods. After co-registration, masks of every ROI were applied to perfusion maps and average CBF and CBV values per ROI were computed. Diffusion-weighted images were processed using version 4.1 of the software package FSL. Parcellation of the individual FA maps into different tracts was based on the ICBM-DTI-81 white matter labels atlas.

Results

Normalization of CBF parametric maps based on whole-brain cortical GM led to a more sensitive detection of perfusion changes in early AD (MCI-c and AD patients) than normalization based on using the cerebellum or whole-brain WM as the reference region; therefore, the cerebellum is not necessarily the optimal reference region in MRI studies for AD. In the MCI-c group we observed a significant decrease in CBF in the bilateral parietal lobes and a significant increase in CBF in the right medial temporal lobe. We found a negative correlation between CBF values and mean cortical thickness in the right parahippocampal gyrus that suggests an increase of CBF dependent on cortical atrophy in pre-dementia stages of AD. In the MCI-c group, perfusion deficits were detected as CBF decrease but not as CBV decrease. Therefore, CBF maps characterize perfusion abnormalities in pre-dementia stages of AD better than CBV maps. We did not find correlation between CBF deficits in parietotemporal and frontal cortices and cortical thinning in the medial temporal lobes in either the MCI-c or the AD groups. Therefore, parietotemporal and frontal hypoperfusion seem to be not directly related to medial temporal atrophy. The MCI-c group showed a high correlation between microstructural changes in the parahippocampal WM fibers and perfusion deficits in the parietal lobes, which may support the existence of a disconnection syndrome that could begin in pre-dementia stages of the disease. In the AD group, the lack of correlation between CBF values in parietotemporal and frontal cortices with FA in parahippocampal and cingulate WM fibers suggests that perfusion deficits in this group could not depend on a disconnection syndrome. The AD group did not show any significant correlation between CBF in hypoperfused regions and FA in the WM tract studied. In this case, factors other than disconnection syndrome may be involved in perfusion deficits in this group. We did not find correlation between cortical thinning in the medial temporal lobes and FA decrease in WM tracts of the limbic system in any group.

Conclusions

1) We found a reference region for intensity normalization of perfusion parametric maps (CBF) obtained with MRI that makes it easier to find hemodynamic changes in early AD patients. Among the three reference regions studied (cerebellum, whole-brain WM and whole-brain cortical GM), whole-brain cortical GM was found to be the optimal reference region for normalization of perfusion maps:

• The mean CBF values for total cortical GM showed less bias between pathological groups and controls.

• Normalizing by whole-brain cortical GM showed the highest reduction of variability in intensity.

• Normalization by the whole-brain cortical GM allowed the detection of a greater number of brain regions with hemodynamic changes in patients with early AD.

• The pattern of hemodynamic alterations found after normalization by the whole-brain cortical GM showed a greater consistency with the clinical interpretation of pathology.

2) CBF is an earlier biomarker of hemodynamic abnormalities than CBV in the prodromal stage of AD.

• MCI-c patients showed significant differences for CBF values but not for CBV values.

• AD patients with mild dementia showed significant differences for CBF values but also for CBV.

• Neither CBF nor CBV data showed correlation with atrophy in those brain regions where atrophy and hemodynamic alterations coexisted.

• MCI-c patients showed a strong correlation between increased CBF and loss of cortical thickness in the right parahippocampal gyrus.

3) The decrease in blood perfusion in the parietal regions of MCI-c patients seems to be related to the damage of WM fibers connecting these regions to the medial temporal lobe, thus supporting the disconnection hypothesis. In contrast, in AD patients, hypoperfusion in the parietotemporal and frontal cortices showed no relationship with the damage in these WM fibers, suggesting a different etiology for these perfusion abnormalities.

• Both MCI-c and AD patients showed microstructural changes in WM fibers of some tracts of the limbic system and in some regions of the corpus callosum, suggesting a physical alteration of the cortico- cortical connections within and between brain lobes.

• We did not find correlation between CBF decrease in parietotemporal and frontal cortices and cortical thinning in atrophied regions of the medial temporal lobes either in MCI-c or AD groups.

• In the MCI-c group, blood perfusion deficits in the parietal cortex showed a strong correlation with the microstructural changes of the WM fibers that connect hypoperfused regions with atrophied regions of the medial temporal lobes.

• The lack of correlation between mean cortical thickness in the medial temporal lobes and the FA in WM tracts of the limbic system in both patients groups suggests that microstructural changes in these tracts are not directly related to cortical atrophy in the medial temporal lobes.

1 INTRODUCCIÓN

Con el avance de los sistemas sanitarios y el aumento de la esperanza de vida, las enfermedades asociadas a la vejez, como las demencias, se han convertido en un problema social. Un reciente estudio epidemiológico del año 2013 ha estimado una prevalencia global, mundial, de 35.6 millones de afectados en el año 2010, con cerca de 5 millones más de casos por año. Dado que el principal factor de riesgo es la edad, se calcula que con el envejecimiento de la población, principalmente en los paises desarrollados, la prevalencia se duplicará cada 20 años superando los 100 millones de afectados para el 2050 (Prince et al., 2013). Esta alta prevalencia supondrá un alto coste económico para las sociedades de los países desarrollados. Otro reciente estudio estima que para el año 2040 el coste monetario anual dedicado a estos pacientes en EEUU se incrementará en un 80% respecto a los cerca de 200 millones de dólares empleados en el año 2010 (Hurd et al., 2013).

Dentro de los distintos tipos de demencias, la enfermedad de Alzheimer (EA) es la más común, atribuyéndosele, aproximadamente, el 70% de los casos de demencia (Reitz et al., 2011). Esta enfermedad afecta en torno al 1% de la población mayor de 65 años y hasta el 40% de población de edad superior a los 85 años (Cummings and Cole, 2002). La EA es un trastorno neurodegenerativo que comienza con dificultades leves de memoria y progresa lentamente hacia una alteración significativa de la memoria, la función ejecutiva, las habilidades visuoespaciales, el lenguaje y otros campos de la cognición. Este trastorno implica una pérdida de la independencia de los pacientes, suponiendo una carga emocional y económica para sus familias. La progresión de la enfermedad es gradual y los pacientes conviven con ella entre 8 y 10 años tras la manifestación de los síntomas (Carr et al., 1997). Entender los procesos patológicos que desencadenan la enfermedad ayudará a mejorar el diagnóstico precoz y sus posibles tratamientos, evitando quizá el incremento exponencial de afectados que pronostican los estudios epidemiológicos.

1.1 Etiopatología de la enfermedad de Alzheimer

Desde que en 1906 Alóis Alzheimer describiera por primera vez esta enfermedad como "Proceso patológico peculiar grave del córtex cerebral" (Alzheimer, 1907), numerosos grupos de investigación han tratado de encontrar las causas que originan este tipo de demencia.

A nivel patológico, la EA se caracteriza por la pérdida de neuronas corticales implicadas en los procesos cognitivos, inicialmente en la región medial de los lobulos temporales y posteriormente en las cortezas de asociación y el resto del neocórtex. La alteración neuronal que desencadena la muerte celular parece deberse tanto a mecanismos intracelulares (ovillos neurofibrilares) como extracelulares (placas amiloides) (Braak and Braak, 1991) (Figura 1.1).

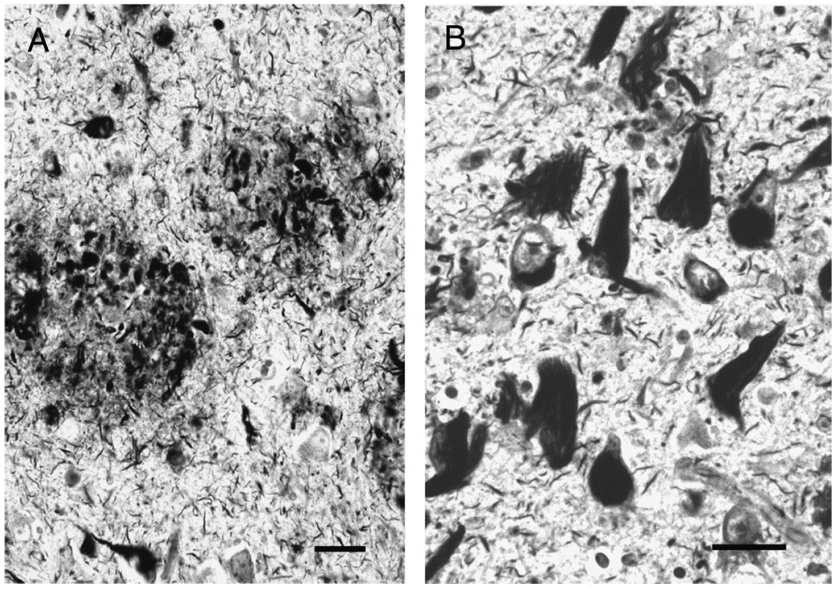

Figura 1.1: (A) Placas neuríticas constituidas por agregados extrecelulares de proteina β-amiloide. (B) Ovillos neurofibrilares constituidos por polímeros intracelulares de proteína tau. Barras de escala = 25µm. Figura extraída de Nelson y cols., 2009 (Nelson et al., 2009).

Además de la aparición de estos ovillos y placas, numerosos estudios (de la Torre, 2002, 2004; Zlokovic, 2005, 2011, 2013), incluidos estudios post-mortem (Chui et al., 2006; Jagust et al., 2008; Tian et al., 2006), han mostrado importantes alteraciones cerebrovasculares asociadas a la EA. Estos hallazgos han llevado a pensar en la EA como una patología de origen "mixto" neurológico y vascular.

1.1.1 Ovillos neurofibrilares

Los ovillos neurofibrilares (NFTs, *neurofibrillary tangles*) están formados por cúmulos de filamentos helicoidales pareados (PHFs, *paired helical filaments*) constituidos por la proteína tau hiperfosforilada. En condiciones normales, esta proteína aparece asociada al citoesqueleto, jugando un papel principal en el ensamblado de microtúbulos y en su estabilización frente a la inestabilidad dinámica. Además, también tiene la capacidad de establecer puentes entre microtúbulos y otros filamentos del citoesqueleto. En un cerebro normal, existe un equilibrio entre las fosforilaciones y desfosforilaciones de tau que modula la estabilidad del citoesqueleto y, por tanto, la morfología axonal. En el caso de la EA, la proteína tau pierde su capacidad de asociación al citoesqueleto y genera los PHFs. Estas formaciones filamentosas alteran la funcionalidad neuronal, lo que lleva a la muerte celular (Maccioni et al., 2001).

La evolución de la dispersión de los NFTs en el cerebro se ha descrito en seis etapas. En la etapa I aparecen en la región transentorrinal y progresan hacia la región entorrinal e hipocampal en la etapa II. Estas dos etapas se dan en una fase presintomática de la enfermedad. Las etapas III y IV se caracterizan por la amplia afectación de la región entorrinal, amígdala, y formación hipocampal. Esto genera una interrupción del transporte de información de doble sentido entre la neocorteza y la formación hipocampal. También se encuentran afectados varios núcleos subcorticales con proyecciones difusas hacia la corteza. Los pacientes en estas etapas pueden presentar un deterioro cognitivo leve (DCL). En la etapa V, la afección se extiende a la mayoría de las regiones de la corteza cerebral, desde las áreas de asociación hacia las áreas primarias. En la etapa VI se ven afectadas las áreas sensoriales primarias. Estas dos últimas etapas (V y VI) se caracterizan por una demencia grave (Braak and Braak, 1991; Delacourte, 1999).

1.1.2 Placas neuríticas o amiloides

Las placas neuríticas (NPs, *neuritic plaques*) consisten en agregados extracelulares de proteina *β*-amiloide. Estas placas están intimamente asociadas con la distrofia de neuritas (axones y dendritas) y la presencia de microglía reactiva (Petrella et al., 2003). La proteina *β*-amiloide se genera mediante la proteolisis de la proteina precursora de amiloide (APP, *amyloid precursor protein*), una glucoproteina que se encuentra en altas concentraciones en la membrana celular de todas las células de mamíferos, pero especialmente en células neuronales. Hasta el momento, la función de la APP no se conoce con claridad, aunque se le han atribuido diversas funciones como adhesión celular, neuroprotección o neurotrofismo. Las enzimas responsables de la proteolisis de la APP son la α, β y γ secretasas. Estas generan polipéptidos solubles *β*-amiloide (1-40 péptidos) y polipéptidos con una mayor capacidad de agregación *β*-amiloide (1-42 péptidos). La secreción de *β*-amiloide al espacio extracelular es algo normal, pero el incremento de la producción de amiloide en su forma menos soluble (1-42 péptidos) favorece la precipitación, agregación y la progresiva deposición en forma de placas en el cerebro (Maccioni et al., 2001).

Se han descrito tres etapas en la evolución de la deposición de placas. La etapa I se caracteriza por la deposición en la corteza entorrinal. Durante la etapa II se extienden hacia la formación hipocampal. Finalmente aparecen en todo el neocórtex durante la etapa III. En cualquier caso estas placas no parecen ser específicas de la enfermedad de Alzheimer pues se han observado también en ancianos que no presentan evidencias de trastorno cognitivo (Bennett et al., 2006; Davis et al., 1999; Knopman et al., 2003; Price and Morris, 1999; Rentz et al., 2010; Tomlinson et al., 1968; Villemagne et al., 2011).

1.1.3 Alteraciones cerebrovasculares asociadas a EA

Estudios neuropatológicos han demostrado que sólo el 20% de los casos de Alzheimer presentan exclusivamente patologías neurológicas propias de la EA (NP y NFTs), presentando el porcentaje restante también alteraciones cerebrovasculares (Henry-Feugeas, 2008). Además, algunos estudios han observado un mayor riesgo de padecer

Alzheimer en pacientes con enfermedades cerebrovasculares (Duron and Hanon, 2008; de la Torre, 2002, 2004), lo que podría indicar cierta relación entre ambos sucesos patológicos. Según algunas hipótesis, habría una estrecha relación entre la neuropatología de la EA y ciertas alteraciones cerebrovasculares, como consecuencia del efecto "tóxico" por una hipoxia prolongada debida a las alteraciones en la microvasculatura. La hipoxia crónica parece desempeñar un papel impotante en la deposición de β-amiloide y , por tanto, en la formaciónde placas amiloides. Se especula también con la posibilidad de que estas placas neuríticas, a su vez, induzcan una cascada neurotóxica en la célula nerviosa, que produciría la formación de ovillos neurofibrilares y la muerte celular (Henry-Feugeas, 2008, 2009). Por otro lado, el descenso de β-amiloide (1-42 péptidos) en el líquido cefalorraquídeo (suponiendo una mayor deposición de amiloide en forma de placas) se ha relacionado con marcadores de disfunción del efecto "windkessel" (efecto basado en la capacidad de distensibilidad arterial, gracias al cual el flujo sanguíneo dentro de la circulación mantiene una constante), como la leucoaraiosis. La leucoaraiosis (degeneración de sustancia blanca por microangiopatías) está relacionada con pérdidas cognitivas y puede estár relacionada con affecciones corticales difusas observadas en la EA (Bech-Azeddine et al., 2007; Stenset et al., 2006). Otra alteración cerebrovascular frecuente en pacientes de EA es la angiopatía cerebral amiloide (CAA, *cerebral amyloid angiopathy*), que aparece en más del 80% de los pacientes. La CAA se produce como consecuencia de la deposición de β-amiloide en las túnicas medias y adventicias de las arterias y arteriolas cerebrales, y produce un efecto tóxico directo sobre las células de músculo liso de estos pequeños vasos. Esta deposición de β-amiloide tiene como consecuencia la degeneración de la barrera hematoencefálica y es la principal causa de pequeñas hemorragias que se producen en torno al 30% de los pacientes de EA (Zlokovic, 2011). Por razones que aún se desconocen, la CAA afecta principalmente a la arteria posterior cerebral, por lo que sus efectos se producen fundamentalmente en la región occipital del cerebro (Smith and Greenberg, 2009). A consecuencia de estos diversos hallazgos se ha empezado a conceder una mayor importancia al papel de las alteraciones cerebrovasculares en la EA.

Por otro lado, los pacientes de Alzheimer también presentan pérdidas de perfusión sanguínea que podrían deberse a la pérdida de actividad neuronal y por tanto a una menor tasa metabólica (Jakovcevic and Harder, 2007). Los astrocitos parecen tener la capacidad de regular el flujo sanguíneo en función de los requerimientos energéticos de las neuronas (Petzold and Murthy, 2011). Por este motivo, el estudio de la hemodinámica cerebral podría aportar información indirecta de la pérdida de funcionalidad neuronal en estos pacientes.

1.2 Fases de la EA e importancia de un diagnóstico temprano

Considerando el impacto socieoeconómico que tiene la EA en los ancianos y en sus familias urge la necesidad de encontrar algún tratamiento para ralentizar, parar e incluso prevenir los síntomas de la EA lo antes posible. Aunque, hasta hace unos años, los tratamientos para el Alzheimer se han centrado en terapias cognitivas, están empezando a aparecer terapias farmacológicas contra el avance de la enfermedad (Ballard et al., 2007; Lyseng-Williamson and Plosker, 2002). En este sentido, resulta crucial un diagnóstico precoz para ralentizar su avance lo antes posible, preservando la integridad de las funciones cognitivas del paciente (DeKosky and Marek 2003). La EA tiene una fase preclínia donde aparece un DCL no demente y otra fase clínica que coincide con la manifestación de los primeros síntomas de demencia. Dentro de la fase clínica, la EA se puede categorizar como demencia leve (fase temprana), moderada (fase intermedia) o grave (fase tardía). El diagnóstico debería hacerse preferiblemente antes de la aparición de la fase de demencia, para así poder iniciar un tratamiento lo antes posible (Petrella et al., 2003).

Dado que el estudio histopatológico que permite detectar la presencia de NP y NFTs sólo se realiza post-mortem (excepto en casos muy limitados mediante biopsia cerebral), la EA ha evolucionado hacia una entidad predominantemente clínica, con un diagnóstico probabilístico de “EA probable” (Dubois et al., 2010). El criterio para el diagnóstico clínico de EA fue establecido por el NINCDS (National Institute of Neurological and Communicative Disorders and Stroke) y el ADRDA (Alzheimer’s disease and Related

disorders Associations) en 1984 (McKhann et al., 1984). También en esta fecha se reconoció el componente vascular de la EA (Reitz et al., 2011).

Los criterios para el diagnóstico están basados principalmente en evidencias clínicas (alteraciones cognitivas) y en los resultados de técnicas de neuroimagen que evalúan el grado de atrofia tisular y las alteraciones del metabolismo celular. También se utilizan técnicas de laboratorio como el análisis de β-amiloide 42 y proteína tau en líquido cefalorraquídeo (LCR), que han demostrado una alta sensibilidad aunque moderada especificidad para la detección de la EA. Uno de los problemas que presenta este análisis es que no parece haber cambios longitudinales en la proporción de estos compuestos en el LCR con la evolución de la enfermedad, por lo que no serían buenos biomarcadores para la progresión de la enfermedad (Stefani et al., 2009; Stenset et al., 2006). En cuanto a las técnicas de neuroimagen, las más empleadas para evaluar el grado de atrofia son tomografía computarizada (CT, *computerized tomography*) y la resonancia magnética (RM) estructural. Para evaluar la disminución del metabolismo de glucosa se emplea la tomografía por emisión de positrones (PET, *positron emision tomographty*). Para evaluar el grado de perfusión sanguínea se han empleado tradicionalmente la PET y la tomografía computarizada de fotón único (SPECT, *single-photon emission computed tomography*), aunque recientemente se ha comenzado a emplear la MR de perfusión como alternativa a las técnicas PET y SPECT.

1.3 Papel de la técnica de Imagen por Resonancia Magnética como marcador de la aparición y progresión de la EA

La imagen por resonancia magnética (MRI, *magnetic resonance imaging*) es una de las modalidades de imagen médica de más reciente aparición y que han experimentado un avance más rápido. Proporciona una buena resolución espacial y un excelente contraste. Se basa en un fenómeno físico descubierto en fechas relativamente recientes (1945) denominado *resonancia magnética nuclear*. Este es un fenómeno por el cual determinados núcleos atómicos son capaces de absorber y emitir energía electromagnética (ondas de radio) de una frecuencia muy precisa (resonancia) cuando se

someten a un intenso campo magnético. La máquina de resonancia genera un potente campo magnético que alinea los espines de los núcleos atómicos. A continuación, la máquina emite un breve pulso de energía de radiofrecuencia. Los protones absorben esta energía a la frecuencia de resonancia, realineándose en un ángulo oblicuo al campo magnético. Tras el pulso magnético, una antena recibe la energía que liberan los núcleos de los átomos excitados al volver al equilibrio. El tiempo de relajación de los núcleos será diferente dependiendo del tejido en el que se encuentren (Gibby, 2005). Aunque hay varios elementos de interés biológico cuyos núcleos presentan el fenómeno de resonancia magnética (hidrógeno, fósforo, sodio, etc.), en los sistemas de imagen para uso clínico se trabaja sólo con el núcleo de hidrógeno por el momento. Las imágenes se obtienen usando un scáner de resonancia magnética. Este genera imágenes digitales en la que cada píxel (unidad de imagen) representa un valor relacionado con el tiempo de relajación del tejido u otros parámetros físico-químicos del mismo.

Una de las mayores ventajas de la RM es que se trata de una técnica no invasiva e inocua, pues no se han descrito efectos nocivos de los campos magnéticos elevados. Por otro lado, los resultados obtenidos hasta la fecha han demostrado la utilidad de los datos obtenidos con esta técnica para realizar diagnósticos en fases iniciales de la EA, que permitirían comenzar cuanto antes con tratamientos específicos para cada patología. De esta manera, no sólo se aumentará la eficiencia de los tratamientos, sino que también mejorarán las circunstancias de los propios pacientes y su entorno familiar.

Además de la imagen estructural, esta técnica de RM presenta muchas variedades de imagen funcional como la RM espectroscópica, que permite obtener información bioquímica de los tejidos, la RM por tensor de difusión (DTI, *diffusion tensor imaging*), que permite evaluar la conservación de los axones, o la RM de perfusión que aporta información de la microvasculatura.

1.3.1 Resonancia magnética estructural

La RM convencional, o estructural, aporta información sobre la localización, el contorno y el tamaño de los distintos tejidos cerebrales. Esta técnica se basa en la composición

diferencial del porcentaje de agua en los distintos tejidos. El estudio de imagen estructural estándar comprende dos tipos de secuencias: ponderadas en T1 y ponderadas en T2. Las secuencias ponderadas en T1 aportan más detalle de los tejidos, mientras que las ponderadas en T2 permiten visualizar mejor los líquidos (Figura 1.2).

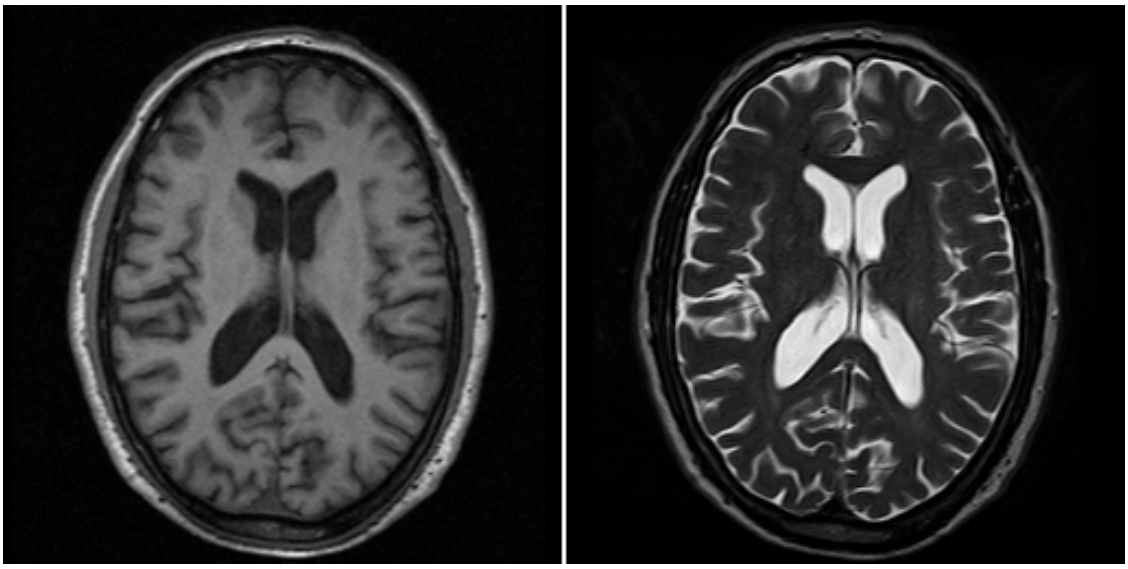

Figura 1.2: Ejemplo de una imagen de resonancia magnética convencional T1 (izquierda) y T2 (derecha).

1.3.1.1 Evaluación de la atrofia cerebral mediante RM estructural

La RM estructural es el método de imagen más empleado en la valoración de la atrofia cerebral en la EA, por encima del CT. Existen estudios post-mortem que han demostrado una alta correlación entre la pérdida de neuronas en los hipocampos, observada en cortes histológicos, y el grado de atrofia observado en los estudios de imagen por RM, validando así esta modalidad de imagen para el estudio de la atrofia en esta enfermedad (Bobinski et al., 2000). Esta técnica se ha propuesto, por tanto, como una posible herramienta para el diagnóstico y seguimiento *in vivo* de la EA (Chan et al., 2003; Vemuri et al., 2008; Zhang et al., 2014).

En los enfermos de Alzheimer se puede observar atrofia en regiones específicas como el lóbulo temporal medial, especialmente en la amígdala, el hipocampo y la corteza

entorrinal, una reducción del grosor cortical en el precuneus, cíngulo posterior y regiones parieto temporales, y un incremento del volumen de los ventrículos y del tamaño de los surcos (Ishii et al., 2006). Concretamente, la atrofia cerebral del lóbulo temporal medial ha pasado a ser uno de los biomarcadores más validados para el diagnóstico de la EA (Dubois et al., 2010). Sin embargo, este biomarcador no parece ser lo suficiéntemente específico como para diferenciar la EA de otras situaciones en las que se produce un deterioro cognitivo (Knopman et al., 2001), debido a que la atrofia del lóbulo temporal medial no es específica de esta enfermedad y aparece también en otro tipo de demencias (Barkhof et al., 2007; Bocti et al., 2006), e incluso en la población de edad avanzada sin deterioro cognitivo (De Leon et al., 1997). En cualquier caso la RM estructural es de gran utilidad a la hora de descartar otras posibles causas de demencia como pueden ser factores vasculares (infartos lacunares), hidrocefalia normotensiva, etcétera (Petrella et al., 2003).

1.3.2 Resonancia magnética de perfusión por contraste de susceptibilidad magnética

La resonancia magnética de perfusión por contraste de susceptibilidad magnética (DSC, *dynamic susceptibility contrast*) es una técnica que permite estimar la hemodinámica del lecho capilar de una determinada área cerebral y, por tanto, valorar la microvasculatura parenquimatosa. Se trata de una técnica comparable con la PET, ya que se ha obtenido una concordancia del 78% entre los estudios de perfusión con PET y los estudios de RM de perfusión (González et al., 1995). Con relación a la PET, la medida de perfusión mediante RM presenta la ventaja de un menor coste, una mayor resolución espacial y una mejor aceptación por parte del paciente, puesto que puede efectuarse junto a un estudio convencional de RM sin aumentar de forma significativa el tiempo de estudio, además de ser una técnica que no utiliza radiación ionizante.

Este tipo de estudios proporciona información sobre el funcionamiento de la microvasculatura que irriga el parénquima cerebral, estudiando la llegada del contraste al tejido y su posterior lavado. Se basan en el análisis de la evolución en el tiempo de la intensidad de la señal de cada vóxel (unidad de imagen en 3D) después de la inyección de

un contraste con gadolinio. Las variaciones de la señal pueden modelarse matemáticamente para obtener mapas paramétricos.

Los parámetros de la perfusión que suelen cuantificar mediante este tipo de estudios son fundamentalmente el flujo sanguíneo cerebral (CBF, *cerebral blood flow*), el tiempo medio de tránsito (MTT, *mean transit time*) y el volumen sanguíneo cerebral (CBV, *cerebral blood volume*).

Una definición de estos parámetros es:

CBF: se define como la cantidad de sangre aportada por los capilares de una unidad de tejido por unidad de tiempo; se mide en [ml/100 ml de tejido/min] o [ml/100 g de tejido/min] (Figura 1.3).

CBV: es un indicador de vasodilatación (dado en [ml/100 ml de tejido]), la cual juega un rol importante en garantizar el suficiente flujo sanguíneo al tejido.

MTT: se define como el tiempo medio que tarda la sangre en pasar a través del lecho capilar.

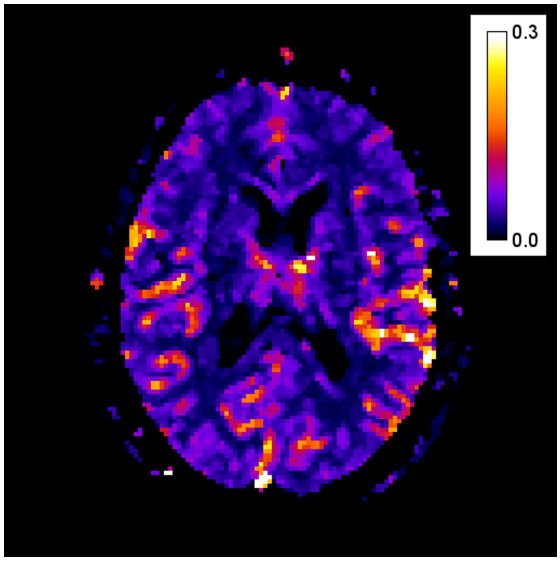

Figura 1.3: Mapa paramétrico de flujo sanguíneo cerebral.

1.3.2.1 Evaluación de la microvasculatura cerebral mediante RM de perfusión

La aplicación de técnicas de perfusión ha permitido alcanzar un mejor conocimiento sobre situaciones en las que la hemodinámica está afectada, como es el caso de pacientes con demencia. El estudio de la hemodinámica cerebral podría ser una herramienta útil para la evaluación y el diagnóstico *in vivo* de la EA (Alsop et al., 2008; Bozzao et al., 2001; Gordon et al., 1998; Uh et al., 2009). Algunos estudios apuntan hacia la hipoperfusión sanguínea cerebral como marcador de progresión desde un estadio de DCL a EA (Caroli et al., 2007). La hipoperfusión podría estar asociada a la formación de placas de β-amiloide. Según estudios post-mortem de material cortical biopsiado en enfermos de Alzheimer, el lecho capilar aparece más laxo cerca de los depósitos de β-amiloide (Kitaguchi et al., 2007). Este hecho podría causar una reducción del CBV que puede afectar a su vez a las medidas de CBF. Por otro lado, la hipoperfusión podría deberse también la reducción de actividad neuronal en regiones donde la integridad del tejido permanece conservada pero que ha perdido aferencias de las regiones dañadas de acuerdo con la hipótesis de la desconexión (Jobst et al., 1992; Matsuda, 2001; Mielke et al., 1996; A. D. Smith, 2002). La hipoperfusión en los pacientes de EA suele aparecer en corteza parietal durante la fase preclínica de DCL y se extiende a cortezas temporal y frontal en etapas más avanzadas de la enfermedad (Johnson et al., 2005).

1.3.3 Resonancia magnética de difusión

El proceso de difusión es el resultado del movimineto translacional aleatorio (o movimiento browniano) de las partículas que componen la materia, impulsado por la energía térmica interna de dichas partículas. Esta propiedad cinética de la materia tiende a igualar las concentraciones de una sustancia en un volumen determinado.

Mediante RM podemos medir la difusión del agua, a partir de la señal de resonancia magnética medida para diferentes direcciones de un gradiente de campo magnético bipolar. La difusividad de las moléculas de agua se verá afectada por barreras físicas como membranas celulares, organelas y macromoléculas (Cooper et al., 1974). La imagen por tensor de difusión o DTI es una modalidad de imagen que permite medir la

direccionalidad de la difusión del agua o asimetría del movimiento del agua en los tejidos (anisotropía). Este método de estimación de anisotropía fue propuesto por Basser y claboradores en 1994 (Basser et al., 1994). En el caso del CSF, el agua se desplaza libremente produciéndose una difusión isotrópica, es decir, idéntica para cualquier dirección. Por el contrario, en la SB, compuesta por densos paquetes de fibras axonales, el agua se mueve más fácilmente en paralelo a las fibras que a través de ellas, por lo que se producirá una difusión anisotrópica paralela a las fibras. De este modo, para cada vóxel de la imagen, en un intervalo de tiempo, el desplazamiento de las moléculas de agua describirá una esfera en el caso de una difusión isotrópica, o un elipsoide en el caso de una difusión anisotrópica. La difusibilidad de una partícula en el medio viene dada por el coeficiente de difusión (D), sin embargo, dado que en la práctica no se puede medir el movimiento browniano de forma independiente de otros movimientos como la microcirculación de la sangre en capilares o movimientos del LCR, lo que se mide es el coeficiente aparente de difusión (ADC, *apparent diffusion coefficient*) (Ito et al., 2002). Otros parámetros frecuentemente empleados en estudios de difusión son: la difusividad media (MD, *mean diffusivity*) y la fracción de anisotropía (FA, *fractional anisotropy*). La MD corresponde al promedio de la difusión de las moléculas de agua independientemente de la direccionalidad del tejido y se ve afectado por el tamaño de los cuerpos celulares y su densidad. La FA refleja el grado de alineamiento de las estructuras celulares y es el principal parámetro de medida de anisotropia (Basser and Pierpaoli, 1996).

1.3.3.1 Evaluación de la microestructura de tractos de SB mediante RM de difusión.

En la EA, el estudio de los cambios de anisotropía se ha focalizado en los estadios prodrómicos y más iniciales de la enfermedad. El daño producido en las fibras de SB se traduce en una reducción de la restricción axonal al movimiento aleatorio de las moléculas de agua, observándose una reducción de la FA en numerosos tractos de SB en estos pacientes. Diversos estudios han demostrado una pérdida de FA en algunos tractos del sistema límbico (cíngulo, parahipocampo y fornix), fibras de asociación (fascículo uncinado y fascículo longitudinal superior) y algunas regiones del cuerpo calloso como el

splenium (Fellgiebel et al., 2008; Mielke et al., 2009; Rose et al., 2000, 2006; Teipel et al., 2007; Zhang et al., 2007).

2 MOTIVACIÓN Y OBJETIVOS

2.1 Motivación

Aunque en la actualidad las técnicas más validadas para el diagnóstico *in vivo* de la EA son la RM estructural y la PET (Dubois et al., 2010), la técnica de RM presenta muchas variedades de imagen funcional menos estudiadas que podrían suponer una herramienta con gran potencial diagnóstico en un futuro. Es el caso de la RM por tensor de difusión que permite evaluar la conservación de las fibras de SB, o la RM de perfusión que aporta información de la microvasculatura cerebral. En los últimos años, se ha concedido una mayor importancia al estudio de las alteraciones hemodinámicas en el cerebro de estos pacientes, ya que parece tener un papel clave en la patogénesis de la enfermedad (de la Torre, 2004; Henry-Feugeas, 2009). Debido a la reciente incorporación de la técnica de perfusión por RM en la valoración de los pacientes de EA, no existe aún información en la literatura sobre ciertos aspectos metodológicos que podrían mejorar su eficacia diagnóstica. No se ha hecho un estudio de validación de una región de referencia para la normalización de intensidad de las imágenes de perfusión, empleándose comunmente el cerebelo en referencia a estudios realizados en PET o SPECT (Bozzao et al., 2001; Harris et al., 1998; Uh et al., 2009). El proceso de normalización es un paso importante en el tratamiento de la imágenes de perfusión pues permite eliminar la variabilidad de intensidad debida a procesos biológicos y experimentales no controlados durante la adquisición y que dificultan la detección de cambios hemodinámicos en estudios comparativos entre pacientes y controles. Tampoco hay estudios comparativos sobre la sensibilidad de los parámetros de perfusión (CBV, CBF) a los cambios hemodinámicos en las distintas etapas de la enfermedad. Dado que el CBF parece ser más sensible que el CBV a los cambios funcionales en las neuronas (Grubb et al., 1974) el CBF podría ser más sensible también en la detección de las anomalías hemodinámicas en las fases más tempranas de la enfermedad, detectando antes cambios funcionales en estos pacientes asintomáticos que el CBV. Por último, el estudio combinado de técnicas de RM (convencional, perfusión y difusión) en la caracterización de pacientes en fases tempranas de la EA podría arrojar luz sobre si las alteraciones hemodinámicas observadas en estos

pacientes tienen o no una relación directa con la atrofia cerebral o los daños en las conexiones neuronales. De acuerdo a la hipótesis de la desconexión (Jobst et al., 1992; Matsuda, 2001; Mielke et al., 1996; A. D. Smith, 2002), la pérdida de perfusión sanguínea en algunas regiones corticales reflejaría una hipoactivación neuronal en dichas regiones corticales como consecuencia de una reducción de "inputs" neuronales desde los lóbulos temporlales mediales, regiones afectadas por la neuropatología en las fases más tempranas de la enfermedad. Una correlación significativa entre la pérdida de perfusión sanguínea en el córtex cerebral y los cambios microstructurales en fibras de SB que conectan las zonas hipoperfundidas con las regiones mediales de los lóbulos temporales podría darnos un indicio de un daño físico en los enlaces entre dos regiones funcionalmente conectadas y una explicación a las alteraciones hemodinámicas, sobre la base de una desconnexión funcional. Hay estudios recientes en los que se han medido variables de perfusión, estructura y difusión en grupos de pacientes con DCL y EA para regiones corticales commúnmente afectadas por la neuropatología de Alzheimer (Zimny et al., 2011, 2013) pero no han medido la relación entre estas variables en distintas regiones de interés de acuerdo a la hipótesis de la desconexión.

2.2 Objetivos

El objetivo principal de esta Tesis Doctoral es estudiar ciertos aspectos metodológicos del procesamiento de imágenes por RM de perfusión que faciliten la detección de alteraciones hemodinámicas cerebrales en las fases tempranas de la EA, y la relación de dichas alteraciones hemodinámicas con los cambios macro y microestructurales que se producen en el córtex cerebral y en los tractos de sustancia blanca respectivamente. Para ello se han propuesto los siguientes objetivos específicos:

- Encontrar una región de referencia para la normalización de intensidad de los mapas paramétricos de perfusión que mejore la detección de diferencias en la perfusión cerebral entre pacientes en fases tempranas de EA y controles en estudios comparativos.

- Comprobar cuál de las variables de perfusión (CBV, CBF) constituye un mejor biomarcador de las alteraciones hemodinámicas en las etapas más tempranas de la enfermedad.

- Comprobar si existe una correlación entre las alteraciones hemodinámicas y la atrofia cortical cuando coincidan en una misma región los dos eventos patológicos.

- Medir el parámetro “fracción de anisotropía” para valorar posibles cambios en la microestructura de los tractos de SB en los pacientes.

- Medir la correlación entre la atrofia cortical en la región medial de los lóbulos temporales y la pérdida de perfusión sanguínea en la corteza parietotemporal y frontal.

- Medir la correlación entre la pérdida de perfusión sanguínea en la corteza parietotemporal y frontal y la pérdida de FA de los tractos que conectan estas regiones corticales con la región medial de los lóbulos temporales.

- Medir la correlación entre la atrofia cortical en los lóbulos temporales mediales y la pérdida de FA de los tractos del sistema límbico.

3 MATERIAL AND METHODS

3.1 Participants

A total of 74 subjects were included for this study. Patient subject were prospectively recruited during routine clinical practice in the behavioural neurology clinic of the Hospital General Universitario Gregorio Marañón by one single senior neurologist with expertise in behavioural neurology. Patients with cognitive impairment were recruited at the stage of mild cognitive impairment (MCI=37) or mild Alzheimer disease (AD=15). Control subjects (n=22) were chosen from volunteers attending the behavioral neurology clinic as patient caregivers and from among researchers' acquaintances. Written informed consent was obtained from all participants and all examinations were performed under a protocol approved by the Hospital General Universitario Gregorio Marañón Ethics Committee.

Every patient was clinically followed at least during 2 years in order to have a progression of their diagnoses. During this clinical follow up, some patients changed their initial diagnosis to normal cognition or other dementias (frontotemporal dementia or Lewy body dementia) (Figure 3.1). Patients were then reorganized into different groups according to their final diagnosis: MCI, MCI converters to AD and mild AD. The specific groups, the number of participants from each group and demographic data for the final sample size will be detailed in each chapter of this doctoral thesis for an easier reading.

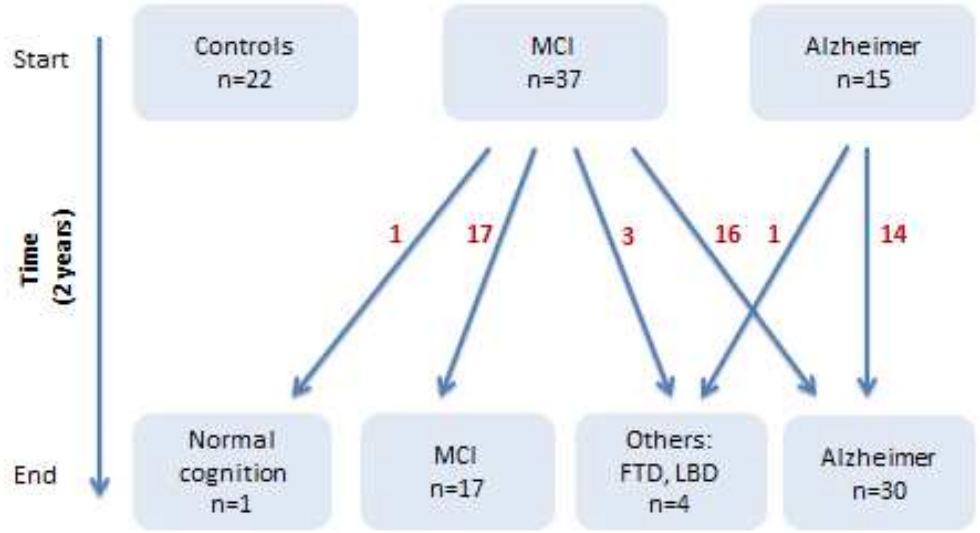

Figure 3.1: Patients classification according to diagnoses progression during 2 years of clinical follow up. MCI: mild cognitive impairment, AD: Alzheimer disease, FTD: frontotemporal dementia. LBD: Lewy body dementia.

3.2 Inclusion criteria for the study

General inclusion criteria were age over 60 years and ability to read and write. All the participants received a formal battery of neuropsychological tests including the California Verbal Learning Test (CVLT) (Delis, et al., 2000), the Frontal Assessment Battery (FAB) (Dubois, et al., 2000), a verbal fluency test (Lezak, et al., 2004), Addrenbrooke's Cognitive Examination (ACE) (Mathuranath, et al., 2000) and the Rey-Osterrieth Complex Figure Test (ROCF) (Spreen and Strauss, 1998). Mini-Mental State Examination (MMSE) was included as part of the ACE (Folstein et al., 1975). In the case of the patients, potential existence of cognitive impairment was investigated by means of a semi-structured interview and a physical and neurological examination. Routine blood determinations, including complete blood count, glucose, creatinine, hepatic enzymes, sodium, potassium, calcium, thyroid-stimulating hormone, B12 and folate, were obtained in the MCI and AD groups to detect causes of cognitive impairment other than AD.

Subjects were excluded if they presented any medical, psychiatric, or neurological condition (except the possibility of AD) that could affect cognition. Patients were not receiving medication for AD at the time of study.

The specific criteria for inclusion in each of the study groups are detailed in the following paragraphs.

MCI group: MCI was diagnosed using the criteria of Winblad et al. (Winblad et al., 2004), which extend the criteria of Petersen et al. (Petersen et al., 1999). Criteria included self- and/or informant report of impairment in any cognitive function with preserved basic activities and no (or minimal) impairment in complex instrumental functions. Cognitive impairment had to be supported by an abnormal performance (1-1.5 SD below the expected performance for age and education) in one or more tests from the neuropsychological battery. In addition, MCI patients did not meet the criteria for dementia according to the Diagnostic and Statistical Manual of Mental Disorders (DSM-IV-TR) (American Psychiatric Association, 2000) and were at stage 0.5 in the CDR (Hughes et al., 1982). After 2 years of clinical follow-up, the criteria for MCI persisted in this group.

MCI-converters group: MCI-converters (MCI-c) patients were diagnosed using the same criteria as the group above, but the patients converted to dementia due to AD after 2 years of clinical follow-up and fulfilled the same criteria as the mild AD group.

Mild AD group: Probable AD was diagnosed using the criteria established by the National Institute of Neurological and Communicative Disorders and Stroke – Alzheimer Disease and Related Disorders Association (NINCDS–ADRDA) (McKhann et al., 1984). Hence, deterioration in memory and other cognitive functions had to be documented, and instrumental activities of daily living had to be affected. The diagnosis of mild AD was always supported by a score of 1 (i.e., mild dementia) in the CDR.

Control group: subjects were cognitively normal, and performed within the normal limits in the cognitive tests, according to age and education. They showed a score of 0 in the Clinical Dementia Rating (CDR) and a score above 24 in the MMSE.

3.3 Image acquisition

MRI data were acquired using a Philips Intera 1.5 T scanner (Philips Medical Systems, Best, The Netherlands).

The imaging protocol included a volumetric T1-weighted 3D gradient echo, which was used for tissue segmentation (Flip angle=30º; Repetition time [TR]=16 ms, Echo Time [TE]=4.6 ms; matrix size=256x256; FOV=256x256 mm and 100 slices with slice thickness=1.5 mm).

Perfusion-weighted images (PWI) were obtained using an echo-planar imaging sequence (EPI factor=61, Flip angle=40º; TR=1439 ms, TE=30 ms; matrix size=128x128; FOV=230x230 mm; section thickness=5 mm) after injecting a bolus of gadolinium chelate (10 ml of gadobutrol; Gadovist® Bayer-Schering AG, Berlin, Germany) , which was followed by administration of 30 ml of saline solution (4 ml/s). Forty volumes (30 slices each) per subject were obtained during the administration of the gadolinium contrast (automatic injector, 4 ml/s).

Diffusion-weighted images (DWI) were acquired using a single-shot echo-planar imaging sequence with the following parameters: imaging plane, axial; phase encoding direction, A–P; TE =68 ms, TR =11886 ms; flip angle = 90º; EPI factor =77; number of slices =60; interslice gap =0 mm; voxel size =2x2x2 mm; and matrix size 128x128. A single non–diffusion-weighted image and 16 diffusion weighted images were acquired. The diffusion weighted images were obtained for b-values of 0 and 800 s/mm^2 over 16 non-collinear directions following an icosahedral scheme.

3.4 Image processing

3.4.1 Structural image processing

Brain mask extraction

Brain masks were estimated from skull-stripped baseline images generated using the VBM8 toolbox (available at: http://dbm.neuro.uni-jena.de/vbm) for the SPM8 package (Wellcome Trust Centre for Neuroimaging, London, UK; available at: http://www.fil.ion.ucl.ac.uk/spm). This algorithm produces a skull-stripped 'p0' image that consists of brain tissue classified into GM, WM and cerebrospinal fluid (CSF). The 'p0' images were binarized and visually inspected to correct brain segmentation errors. The skull was removed manually if necessary.

FreeSurfer processing

T1-weighted images were processed using the FreeSurfer package (version 4.5.1, http://surfer.nmr.mgh.harvard.edu) to estimate cortical gray matter volume and mean cortical thickness per ROI. Brain mask images obtained from the VBM8 toolbox were introduced into the default FreeSurfer processing pipeline because they provide more accurate skull stripping.

The white and gray cortical surfaces were reconstructed from the raw unaligned images in native space, with the methods described by Fischl and Dale (Fischl and Dale, 2000) and Dale et al. (Dale et al., 1999) (Figure 3.2). The reconstruction process was supervised and corrected when necessary by an operator blind to the subject's diagnosis. The measurement technique used by FreeSurfer has been validated using histological measurements (Rosas et al., 2002) and manual measurements (Kuperberg et al., 2003).

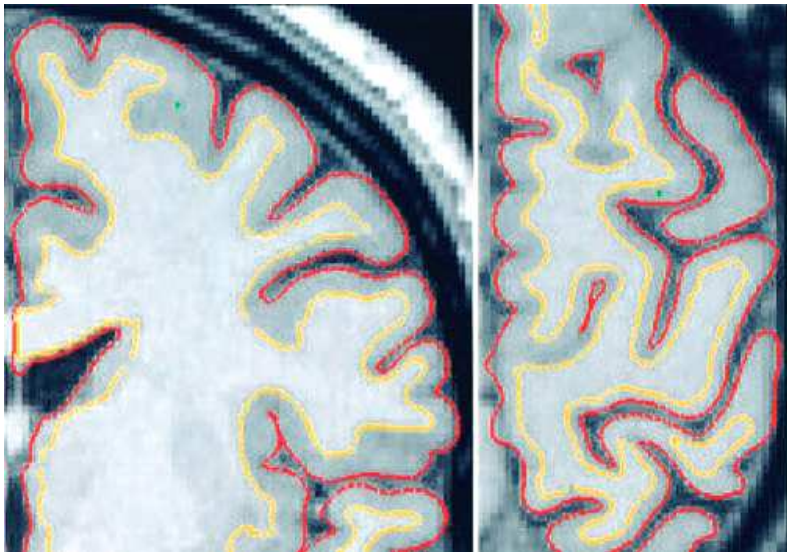

Figure 3.2: Coronal slice (left) and axial slice (right) of the left hemisphere showing GM/WM interface (yellow) and GM/CSF interface (red). Image from (Fischl and Dale, 2000).

Cortical GM volume and mean cortical thickness for different regions of interest (ROIs) were obtained by applying the Desikan-Killiany atlas (Desikan et al., 2006) (Figure 3.3). Whole-brain WM, amygdalae, hippocampi and cerebellum were segmented according to (Fischl et al., 2002).

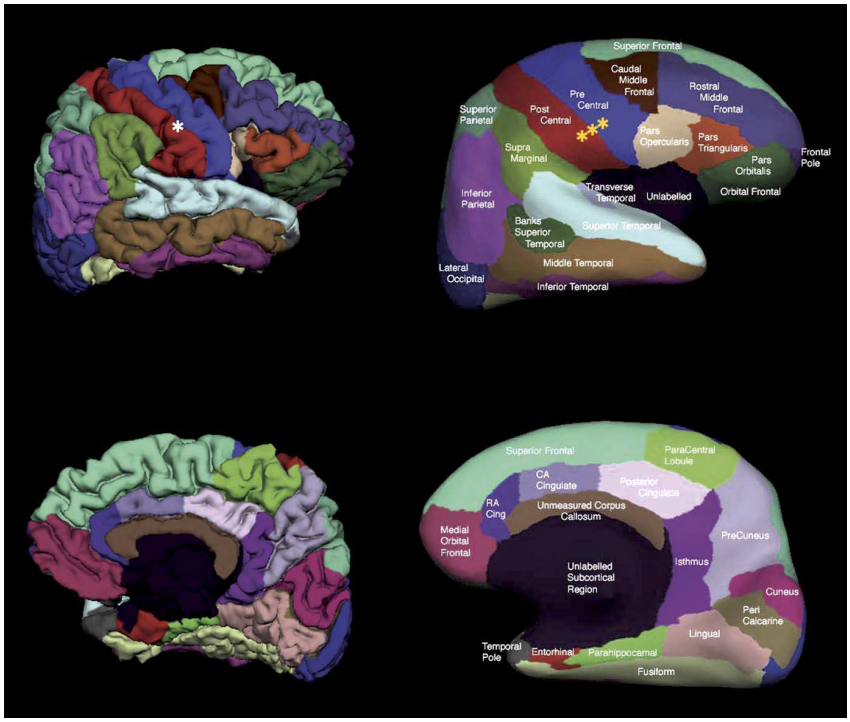

Figure 3.3: Desikan-Killiany atlas used for cortical parcellation into gyral based regions of interest (Desikan et al., 2006).

3.4.2 PWI processing

CBF and CBV maps were obtained according to the following equation:

$$CBF = \frac{CBV}{MTT}$$

Where

$$CBV = \frac{\int C_m(t)}{\int AIF(t)}; MTT = \frac{\int C(t)}{C_{\max}}$$

In the previous equation, there are two different concentrations: the concentration that can be measured directly from the image data ($C_m(t)$) and the concentration resulting from a deconvolution operation with the arterial input function (AIF). Both concentrations can be expressed mathematically as

$$C_m(t) = -\ln\frac{S(t)}{S_0}; C(t) = C_m(t) \otimes^{-1} AIF(t)$$

Where S(t) is the MRI image signal, S_0 is the signal in the first six frames, when the contrast bolus still is not present and $\otimes^{-1}$ represents the deconvolution operation.

The AIF was calculated automatically using the method detailed in Rempp et al. (Rempp et al., 1994). In order to remove noise and other undesired second-order effects, the contrast curves where fitted to a gamma function according to the linearization method proposed in Li et al. (Li et al., 2003).

In CBV maps, pixels with signal intensity higher than the 98th percentile of the brain values were excluded from all regional analyses, as they probably included blood vessels.

CBF and CBV parametric maps of PWI were co-registered with T1-weighted images using mutual information methods (Collignon et al., 1995). Gyrus-based ROI masks, obtained from the Desikan-Killiany atlas, were then applied to CBF perfusion maps and the average CBF and CBV value per ROI was computed.

3.4.3 DWI processing

Diffusion-weighted images were processed using version 4.1 of the software package FSL (FMRIB Software Library, FMRIB, Oxford, UK) (Smith et al., 2004).

For each subject, the 16 diffusion-weighted volumes acquired were co-registered to the b0 image using FLIRT (FMRIB's Linear Image Registration Tool) to correct for possible Eddy-current induced distortion and subject motion. A brain mask was created from the first b0 image using BET (Brain extraction Tool) (S. M. Smith, 2002) and FDT (FMRIB's Diffusion Toolbox) (Behrens et al., 2003) was used to fit the tensor model and to compute the FA maps. Parcellation of the individual FA maps into different tracts was based on the *ICBM-DTI-81 white matter labels atlas,* which is one of the standard atlases available in FSL (Mori et al., 2008; Wakana et al., 2004). We extracted the mean FA values of each tract-based ROI.

4 IS THE CEREBELLUM THE OPTIMAL REFERENCE REGION FOR INTENSITY NORMALIZATION OF PERFUSION MR STUDIES IN EARLY ALZHEIMER'S DISEASE?

This chapter has been published as original article: PLoS One. 2013 Dec 27;8(12):e81548. doi: 10.1371/journal.pone.0081548

4.1 Abstract

The cerebellum is the region most commonly used as a reference when normalizing the intensity of perfusion images acquired using magnetic resonance imaging (MRI) in Alzheimer's disease (AD) studies. In addition, the cerebellum provides unbiased estimations with nuclear medicine techniques. However, no reports confirm the cerebellum as an optimal reference region in MRI studies or evaluate the consequences of using different normalization regions. In this study, we address the effect of using the cerebellum, whole-brain white matter, and whole-brain cortical gray matter in the normalization of cerebral blood flow (CBF) parametric maps by comparing patients with stable mild cognitive impairment (MCI), patients with AD and healthy controls. According to our results, normalization by whole-brain cortical gray matter enables more sensitive detection of perfusion abnormalities in AD patients and reveals a larger number of affected regions than data normalized by the cerebellum or whole-brain white matter. Therefore, the cerebellum is not the most valid reference region in MRI studies for early stages of AD. After normalization by whole-brain cortical gray matter, we found a significant decrease in CBF in both parietal lobes and an increase in CBF in the right medial temporal lobe. We found no differences in perfusion between patients with stable MCI and healthy controls either before or after normalization.

4.2 Introduction

Alterations in cerebral hemodynamic processes are thought to be involved in the pathogenesis of Alzheimer's disease (AD) (Henry-Feugeas, 2009; Nagata et al., 2000; Zlokovic, 2011). Furthermore, a correspondence has been demonstrated between decreased cerebral perfusion and neuronal deactivation, purportedly as a consequence of neurovascular coupling (Lecrux and Hamel, 2011; Paulson et al., 2010). Regional cerebral perfusion is associated with tissue metabolic requirements (González et al., 1995). This physiological mechanism may underlie the association between perfusion deficits in the parietotemporal regions and rapid cognitive decline in AD patients (Hanyu et al., 2010). Consequently, measurement of cerebral perfusion using functional imaging may provide useful information for early detection and tracking of AD. Classically, this assessment has been carried out using nuclear medicine techniques, such as positron emission tomography (PET) or single-photon emission computed tomography (SPECT). However, MRI was recently proposed as a potentially useful tool for the evaluation of cerebral perfusion in AD patients (Petrella et al., 2003). Dynamic susceptibility contrast (DSC) MRI is the most widely used perfusion-weighted MRI technique. DSC-MRI also has the advantages of shorter acquisition time, lower cost and no need for ionizing radiation. In addition, in contrast to PET and SPECT, structural and perfusion MRI metrics are easily obtained in the same scan session, thus facilitating clinical routine and patient comfort. However, perfusion MRI is affected by wide physiological variability in perfusion measurements across subjects. This variability, which is due to uncontrolled biological and experimental factors (Diamant et al., 2002), makes it difficult to detect group differences, especially in small samples. In order to achieve more sensitive detection of disease-dependent patterns of altered perfusion, variability can be improved by normalizing data before performing comparative analysis.

The most widely used intensity normalization method computes the ratio of a region of interest (ROI) value to the average perfusion value of all voxels within a reference region.

In nuclear medicine studies, the cerebellum, whole-brain gray matter (GM) and whole-brain white matter (WM) have traditionally been considered good reference regions for intensity normalization (Borghammer et al., 2008). The cerebellum is the most commonly used reference region in SPECT perfusion studies in AD patients, since it has been reported to provide unbiased estimations (Karbe et al., 1994; Soonawala et al., 2002; Talbot et al., 1994). The idea that the cerebellum remains unaffected by AD is controversial, since some authors have reported reduced function in this region in late dementia, suggesting that normalization by this region in advanced AD may lead to errors (Ishii et al., 1997). Using DSC-MRI, other authors recently observed a significant decrease in cerebral blood flow (CBF) in the cerebellum of AD patients (Hauser et al., 2013).

The cerebellum is also the most widely used region for normalization in perfusion-weighted MRI studies of patients with AD (Bozzao et al., 2001; Harris et al., 1998; Uh et al., 2009), although the visual cortex (Alsop et al., 2008), basal ganglia (Alsop et al., 2000) and primary motor cortex (Johnson et al., 2005) have also been used. In MRI studies, no reports confirm that the cerebellum is an optimal reference region for normalization or evaluate the consequences of using different normalization regions in perfusion-weighted MRI measurements.

In this study, we address the effect of using different regions for normalization in an analysis of CBF parametric maps comparing patients with mild cognitive impairment (MCI), AD patients and healthy controls. For this purpose, we normalized CBF maps by whole-brain cortical GM, whole-brain WM and the cerebellum.

4.3 Participants

The study sample comprised 43 patients and 20 controls. Patients were divided into 2 groups: those with mild cognitive impairment (MCI) (n=15) and those with AD (n=28). The AD group comprised 12 patients recruited with probable AD and mild dementia and 16 subjects recruited at the stage of MCI that converted to dementia due to AD after 2 years of follow-up (MCI-c). Demographic and clinical data of the participants are shown

in Table 4.1. No significant between-group differences were found for any of the variables, except in the MMSE score, which was lower in the AD group than in the MCI and control groups.

Table 4.1: Demographic and clinical data

	Controls n=20	MCI n=15	Alzheimer n=28
Age in years (SD)	71.65 (7.04)	70.87 (9.71)	74.86 (6.97)
Sex (Female:Male)	11:9	7:8	15:13
Years of education (SD)	9.1 (4.36)	7.07 (3.39)	6.79 (4.07)
MMSE (SD)	27.55 (2.09)	26.20 (1.97)	20.61 (4.08)*

* ANOVA of group differences (p<0.0001). Significant differences were found between the Alzheimer group and the controls, and between the Alzheimer group and the MCI group. MMSE, Mini Mental State Examination; SD, standard deviation.

4.4 Statistical analysis

We used one-way ANOVA to test the hypothesis that no differences existed in mean CBF values in any of the three chosen reference regions between groups (controls, MCI and AD) in order to rule out any between-group bias in reference regions for normalization. We also used ANOVA to test mean CBF values for differences per lobe between groups before and after normalization by the three reference regions. When the result of ANOVA was significant, we used a post hoc procedure (Dunnett's test) to compare means between patients groups and controls and we calculated the effect size (Cohen's coefficient, d) in order to assess the magnitude of those differences. The effect of using different regions for normalization on the intra-group variability of PWI data was assessed through the coefficient of variation (CV). We also estimated the components of variance for the diagnosis group and normalization region to ensure that any reduction in variability after normalization (measured using the CV) was due to a reduction in intra-group variability and not to a reduction in between-group differences. An ANCOVA model including age as covariate was used to test between-group differences in GM volume in the medial temporal cortex, amygdalae and hippocampi. Data were analyzed using Statistical Analysis System (SAS) version 9.0 (SAS Institute Inc., Cary, NC, USA).

4.5 Results

4.5.1 Between-group bias in reference regions

No statistically significant differences were found in mean CBF values between the groups in any of the three reference regions studied. Intra-group variability in CBF intensity values was similar in the three regions: around 40% in the control group and 50% in the MCI and AD groups (Table 4.2).

Table 4.2: Mean CBF values and intra-group variability in intensity for the three reference regions

	Controls n=20		MCI n=15		Alzheimer n=28		ANOVA	
	Mean (SD)	CV	Mean (SD)	CV	Mean (SD)	CV	F	p
CBFcgm	0.11 (0.04)	39.2	0.11 (0.05)	48.8	0.11 (0.05)	49.3	0.03	NS
CBFcer	0.30 (0.12)	41.0	0.29 (0.14)	50.2	0.28 (0.14)	50.5	0.14	NS
CBFwm	0.07 (0.03)	41.7	0.07 (0.03)	50.3	0.06 (0.03)	50.1	0.28	NS

CV, coefficient of variation (%); SD, standard deviation; CBFcgm, cerebral blood flow of whole-brain cortical gray matter; CBFcer, cerebral blood flow of cerebellum; CBFwm, cerebral blood flow of whole-brain white matter; *F*, ANOVA *F* value; *p*, ANOVA *p* value; NS, not significant.

4.5.2 Effects of normalization on between-group analysis

No statistically significant differences between patient groups and controls were detected for absolute mean CBF values in cortical ROIs. Differences in perfusion values between groups were detected only after normalization of data. CBF data normalized by whole-brain cortical GM showed significantly lower CBF mean values in the right and left parietal lobes and higher mean values in the right medial temporal lobe in AD patients than in the control group (Figure 4.1). No significant differences were found for the parietal lobes in AD patients according to whether the cerebellum or whole-brain WM was used as a reference region.

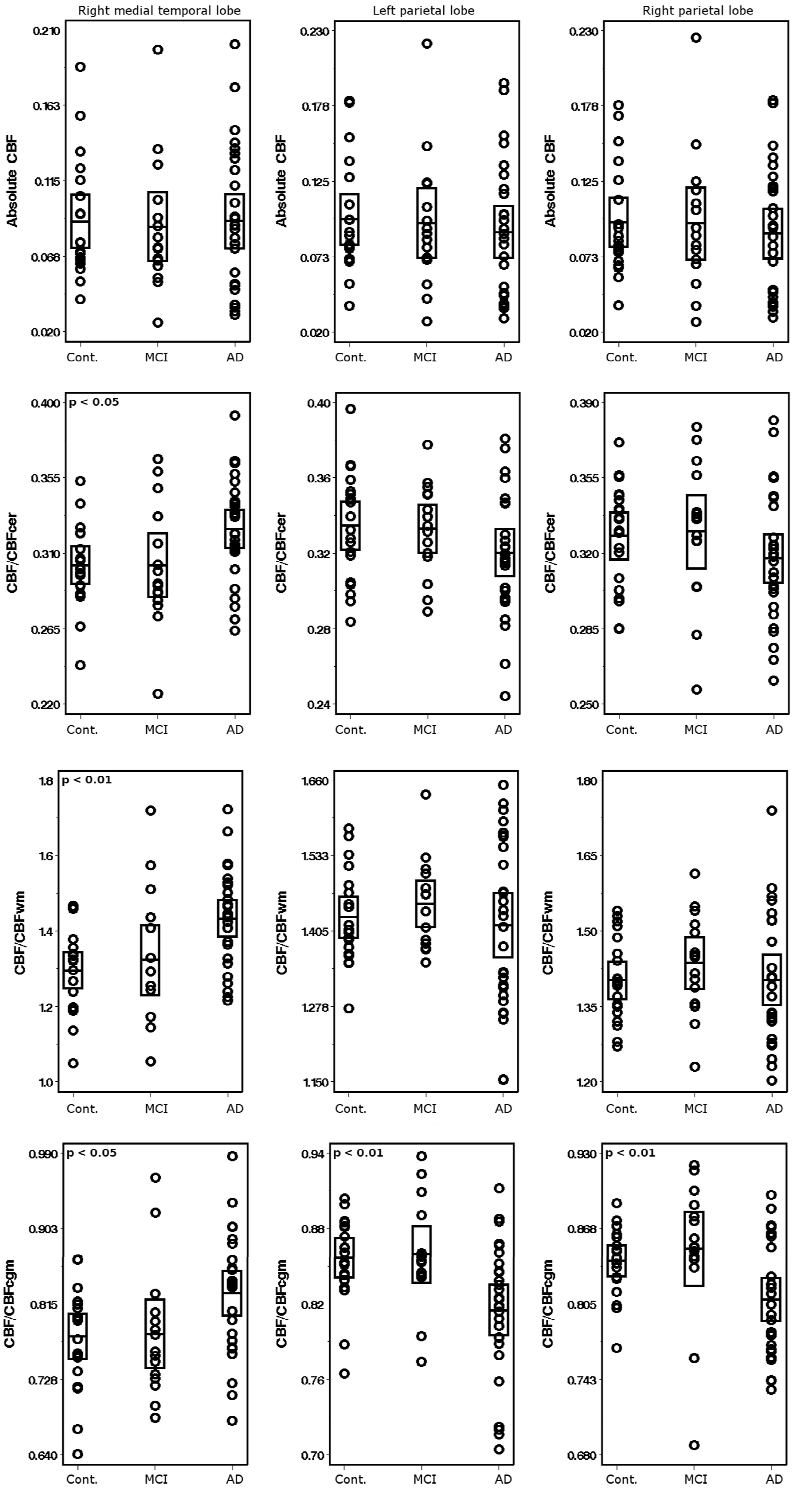
Right medial temporal lobe
Left parietal lobe
Right parietal lobe
Absolute CBF
CBF/CBFcer
CBF/CBFwm
CBF/CBFcgm
p < 0.05
p < 0.01
Cont.
MCI
AD

Figure 4.1: Scatter plots of CBF values for controls, patients with mild cognitive impairment, and patients with Alzheimer's disease in both parietal lobes and right medial temporal lobe. Absolute CBF units are given in ml of blood/100 g of tissue/min. Cont, controls; MCI, mild cognitive impairment; AD, Alzheimer's disease. Bar shows two standard deviations below and above the mean (horizontal line). p, one-way ANOVA p value.

The hyperperfusion pattern in the right medial temporal lobe appeared after normalization regardless of the reference region used; however, statistical significance was higher when normalization was by whole-brain WM than by the cerebellum or whole-brain cortical GM (Table 4.3).

Table 4.3: Dunnett's test *p* values (*p*) and effect size (*d*) of differences between AD patients and controls in mean CBF value for the three reference regions studied.

	Right temporal lobe (medial region)		Right parietal lobe		Left parietal lobe	
	p	d	p	d	p	d
CBFcer	<0.05	0.76	-	-	-	-
CBFwm	<0.01	1.06	-	-	-	-
CBFcgm	<0.05	0.76	<0.05	-0.70	<0.01	-1.17

CBFcgm, cerebral blood flow of whole-brain cortical gray matter; CBFcer, cerebral blood flow of cerebellum; CBFwm, cerebral blood flow of whole-brain white matter; *p*, Dunnett's test *p* value, *d*, Cohen's coefficient.

We found no perfusion differences between the group with stable MCI and controls either before or after normalization. Consistent results were found when the comparative analysis was performed based on cerebral gyri-based ROIs instead of lobe-based ROIs. Compared to controls, AD patients showed higher mean CBF values in the right fusiform gyrus ($p<0.01$) and right parahippocampal gyrus ($p<0.05$) after normalization by the three reference regions. This group also showed lower mean CBF values in the superior parietal gyri (right, $p<0.05$; left, $p<0.01$) and the right precuneus ($p<0.05$) after normalization by whole-brain cortical gray matter. Differences in the left superior parietal gyrus were also found after normalization by cerebellum, although the statistical

significance was weaker ($p<0.05$). No significant differences were observed between the MCI group and controls.

4.5.3 Reduction in intra-group variability after normalization

Intra-group variability in the CBF measurements was considerably reduced after data normalization. Data normalized by whole-brain cortical GM consistently showed the lowest dispersion in every lobe (Table 4.4). The results of the component of variance analysis showed that the variance attributable to the normalization method was considerably larger (over 95%) than the variance attributable to the diagnosis group effect.

Table 4.4: Reduced variability in intensity values after normalization by the three reference regions (coefficients of variation, %).

	Frontal	Parietal	Temporal (lateral)	Temporal (medial)	Occipital
Absolute CBF	46.61	46.96	46.31	45.54	44.47
CBF/CBFcer	8.69	8.76	8.62	10.37	8.72
CBF/CBFwm	7.39	7.40	7.17	11.18	9.82
CBF/CBFcgm	5.54	5.40	5.94	7.98	5.73

CBF, cerebral blood flow; CBF/CBFcgm, CBF values per region of interest normalized by whole-brain cortical gray matter; CBF/CBFcer, CBF values per region of interest normalized by cerebellum; CBF/CBFwm, CBF values per region of interest normalized by whole-brain white matter. Coefficients of variation show bilateral information per lobe in the three groups (controls, MCI and AD).

4.5.4 Medial temporal lobe atrophy

Compared to controls, the AD group showed significantly lower GM volumes in the medial temporal cortex (bilateral), amygdalae and hippocampi. No significant differences in those regions were observed for the MCI group (Table 4.5).

Table 4.5: Dunnett's test *p* values for differences between patients and controls in gray matter volume for the medial temporal lobes.

	Controls-MCI	Controls-Alzheimer
Left temporal cortex	-	0.002
Right temporal cortex	-	<0.001
Left hippocampus	-	<0.0001
Right hippocampus	-	<0.0001
Left amygdala	-	<0.0001
Right amygdala	-	<0.0001

(-) non-significant differences.

4.6 Discussion

The high physiological variability of CBF parametric maps makes it difficult to detect subtle perfusion abnormalities in AD, especially in small samples. Normalization of data based on a reference region usually facilitates the detection of disease-dependent affected regions. However, in comparative analyses, results could vary with the region chosen for normalization. This observation was reported in SPECT studies using 99mTc-hexamethylpropyleneamine oxime (HMPAO), which confirm the cerebellum to be the optimal region for normalization (Karbe et al., 1994; Soonawala et al., 2002; Talbot et al., 1994); however, no studies to date have validated the cerebellum as the optimum normalization region in MRI perfusion studies. The present study shows the effect of using different regions to normalize the intensity of CBF parametric maps acquired by MRI on the results of a comparative analysis between stable MCI patients, AD patients and healthy controls. While SPECT studies confirmed the cerebellum as a valid reference region, our results suggest that it is not optimal in MRI studies in early-stage disease.

4.6.1 Between-group bias in reference regions

A possible disease-associated decrease in absolute CBF values must be ruled out before choosing a region as a reference. The three reference regions chosen for this study did not show any group-related bias. No between-group differences in mean values for absolute CBF data were found in the ANOVA model, and intra-group variability for CBF values was quite similar in all three regions (Table 4.2). An insufficient sample size could be the reason for the undetected differences in global perfusion between patients and controls; in

such cases, the criteria for accepting regions as unbiased is a t value close to zero (Borghammer et al., 2008). In our case, since we compared three groups, we considered an F value close to zero as the criterion for an optimal normalization region. Whole-brain cortical GM showed the F value to be closest to zero (Table 4.2).

4.6.2 Effects of normalization on between-group analysis

Differences in perfusion values between groups were detected only after normalization of CBF data. We observed a statistically significant pattern of hyperperfusion in the right medial temporal lobe of AD patients after normalization. Relatively increased regional CBF in AD patients has been reported for SPECT and is commonly attributed to a reference region that is unsuitable for normalization. Such is the case of Soonawala et al. (Soonawala et al., 2002), who reported increased CBF in the occipital cortex and whole-brain WM using global normalization instead of the cerebellum. Talbot el al. (Talbot et al., 1994) reported the same effect in the frontal lobe when they normalized by the occipital cortex instead of the cerebellum. However, the hyperperfusion pattern observed in the medial temporal lobe in AD patients in our study seems to be independent of the chosen reference region, since the same pattern appeared after normalization by the three regions studied. Increased CBF may suggest compensatory mechanisms (Dickerson and Sperling, 2008) or inflammatory processes. Studies of inflammation in AD have reported activated microglia surrounding amyloid deposits within the brain, which may be responsible for a locally induced chronic inflammatory response (Salminen et al., 2009; Wilkinson et al., 2012).

We also found a significant decrease in CBF in both parietal lobes in the AD group, although only when normalizing by whole-brain cortical GM. Cerebellum-normalized data showed the same hypoperfusion pattern, but group differences did not reach the threshold of statistical significance (Figure 4.1). Similar hypoperfusion patterns in posterior regions of the parietotemporal cortex have been found in SPECT studies (Talbot et al., 1998). According to the disconnection hypothesis (Jobst et al., 1992), the loss of synaptic inputs from the medial temporal lobe in the parietotemporal cortex reduces neuronal activity and blood flow in the region. This may be the reason why perfusion

decreases in very early stages of the disease, when the region has not yet been affected by amyloid plaques (Braak and Braak, 1991). The marked GM volume loss in the medial temporal lobes and the decreased parietal perfusion observed after normalization by whole-brain cortical GM are consistent with the pattern expected for early AD. A similar pattern of hyperperfusion in medial temporal lobes and hypoperfusion in parietal lobes has been described in a CBF study based on arterial spin labeling (ASL) MRI and normalization by the visual cortex instead of the cerebellum (Alsop et al., 2008). This study was based on a sample that was similar to ours in size, MMSE score and age. Although ASL presents methodological differences with respect to DSC (absence of external contrast and longer scan acquisition times, which make ASL more sensitive to patient movement artifacts (Essig et al., 2013), measurements of perfusion by ASL seem to correlate well with DSC perfusion (Huang et al., 2013).

Nevertheless, other MRI studies have reported decreased parietal perfusion when the reference region was the cerebellum (Bozzao et al., 2001; Harris et al., 1998). However, the results may not be comparable to ours, because AD patients were older, with lower MMSE scores, and the variable assessed was cerebral blood volume instead of CBF, which seems to be more sensitive to physiological processes than cerebral blood volume (Grubb et al., 1974).

According to our results, normalization by whole-brain cortical GM enables more sensitive detection of perfusion abnormalities (with a larger number of affected regions in AD patients) than data normalized by cerebellum or whole-brain WM.

We found no differences in perfusion between stable MCI patients and healthy controls before or after normalization. These findings may indicate vascular impairment that is specific to AD and not observed in MCI patients who do not progress to AD. In fact, in the MCI group, we did not observe GM volume loss in the medial temporal lobe, the first region affected by neuropathology in AD. The lack of evidence of AD in this group seems to indicate fulfillment of the specific criteria for MCI according to the new lexicon for Alzheimer's disease proposed by Dubois et al. (Dubois et al., 2010).

4.6.3 Reduction in intra-group variability after normalization

Absolute CBF data dispersion was considerably reduced after normalization by the three reference regions studied. However, normalization by whole-brain cortical GM showed the lowest coefficients of variation in all brain lobes (Table 4.4). The reduced variability in CBF intensity values after normalization could arise from a reduction in intra-group variability, but also from a reduction in between-group differences. The component of variance analysis reveals that reduced variability was due to the first factor. This result could explain why more significant differences were observed between patients and controls after normalization of data. Since intensity variability across subject is the main obstacle to comparative analysis between controls and patients, the greater reduction in variability actually validates whole-brain cortical GM as a good reference region for MRI perfusion studies. One possible explanation is that cortical GM may be subject to sources of variability that are similar to those of the ROIs we studied; therefore, normalization against whole-brain cortical GM could somehow adjust for these hidden factors.

Our study is subject to a series of limitations. Given the differences in spatial resolution between T1 and PWI studies, coregistration may lead to tissue registration mismatch; therefore, some errors in cortical parcellation of CBF maps cannot be controlled. We accepted the results after normalization by whole-brain cortical GM as a more valid perfusion pattern than that obtained after normalizing by cerebellum and whole-brain WM, since similar temporoparietal hypoperfusion patterns have been demonstrated in SPECT studies where AD was confirmed by autopsy (Jagust et al., 2001). The MCI group did not show any pattern of perfusion deficits. This group seems to comply with specific criteria for MCI according to the new lexicon for Alzheimer's disease proposed by Dubois et al. (Dubois et al., 2010). The main strengths of our study are the multimodal nature of the data, the application of an easily reproducible method for brain parcellation and tissue segmentation, and the fact that patients with AD were recruited at a very early stage of the disease, since more than 50% of the patients had prodromal AD (Dubois et al., 2010).

4.7 Conclusions

Our results suggest that normalization of CBF parametric maps based on whole-brain cortical GM leads to a more sensitive detection of perfusion changes in AD patients than when the cerebellum or whole-brain WM is used as the reference region; therefore, the cerebellum is not necessarily the optimal reference region in MRI studies for early-stage AD. When normalizing by whole-brain cortical GM, we found a significant decrease in CBF in both parietal lobes and an increase in CBF in the right medial temporal lobe. This hyperperfusion pattern in the AD group seems to be independent of the chosen reference region. We found no differences in perfusion between the group with stable MCI and healthy controls either before or after normalization, thus suggesting the absence of perfusion abnormalities in this group.

5 CEREBRAL BLOOD FLOW IS AN EARLIER INDICATOR OF PERFUSION ABNORMALITIES THAN CEREBRAL BLOOD VOLUME IN ALZHEIMER'S DISEASE

This chapter has been published as original article: J Cereb Blood Flow Metab. 2014 Jan 15. doi: 10.1038/jcbfm.2013.241.

5.1 Abstract

The purpose of this study was to elucidate whether cerebral blood flow (CBF) can better characterize perfusion abnormalities in pre-dementia stages of Alzheimer's disease (AD) than cerebral blood volume (CBV) and whether cortical atrophy is more associated with decreased CBV or with decreased CBF. We compared measurements of CBV, CBF, and mean cortical thickness obtained from magnetic resonance images in a group of healthy controls, patients with mild cognitive impairment (MCI) who converted to AD after two years of clinical follow-up (MCI-c), and patients with mild AD. A significant decrease in perfusion was detected in the parietal lobes of the MCI-c patients with CBF parametric maps but not with CBV maps. In the MCI-c group, a negative correlation between CBF values and cortical thickness in the right parahippocampal gyrus suggests an increase in CBF that depends on cortical atrophy in pre-dementia stages of AD. Our study also suggests that CBF deficits appear before CBV deficits in the progression of AD, since CBV abnormalities were only detected at the AD stage, whereas CBF changes were already detected in the MCI stage. These results confirm the hypothesis that CBF is a more sensitive parameter than CBV for perfusion abnormalities in MCI-c patients.

5.2 Introduction

Microvasculature abnormalities play a key role in the pathogenesis of Alzheimer's disease (AD) (Zlokovic, 2005). Several neuroimaging studies have pointed to cerebral blood hypoperfusion in the parietotemporal association areas of patients with mild cognitive impairment (MCI) as a predictor of rapid conversion to AD (Matsuda, 2007). However, while there is consensus on the hypoperfusion pattern of parietotemporal areas for AD, results for the medial temporal lobes are inconsistent, probably owing to differences in the spatial resolution of the imaging techniques used (Matsuda, 2007). Blood perfusion abnormalities in patients with AD seem to be associated with local neuronal tissue degeneration caused by the AD neuropathology, but also with reduced neuronal activity in areas functionally connected to those atrophied regions. According to the so-called disconnection hypothesis, functional changes observed in the parietotemporal and frontal regions might be related to reduced neuronal inputs from the medial temporal lobe (Jobst et al., 1992), the primary structure affected by the AD neuropathology. Although perfusion biomarkers are not validated for early diagnosis of AD (Dubois et al., 2010), magnetic resonance imaging (MRI) of perfusion could prove to be a powerful tool in the characterization and tracking of AD and a good alternative to nuclear medicine (Bammer et al., 2005; Gordon et al., 1998).

MRI enables blood perfusion to be assessed through cerebral blood flow (CBF) and cerebral blood volume (CBV). CBV is an indicator of blood vessel lumen size and density, while CBF is the amount of blood reaching the tissue per unit of time and thus contains blood velocity information. Therefore, CBF could be more sensitive to physiological perfusion changes than CBV (Grubb et al., 1974). Most perfusion MRI studies in AD only reported either CBF (Alsop et al., 2008; Johnson et al., 2005) or CBV (Bozzao et al., 2001; Uh et al., 2009); it remains unclear which parameter of the two constitutes an earlier and more sensitive biomarker of AD. To our knowledge, the few studies that measured both variables reported a statistically significant reduction in CBF but a nonsignificant reduction in CBV in the parietotemporal and frontal cortex of AD patients (Hauser et al., 2013; Yoshiura et al., 2009).

We hypothesized that CBF could be a more sensitive indicator of hypoperfusion than CBV in pre-dementia stages of AD, when neuronal activity is already reduced but AD neuropathology has not largely spread. The purpose of this study was to elucidate whether CBF can better characterize perfusion abnormalities in pre-dementia stages of AD than CBV and whether cortical atrophy is more associated with decreased CBV or with decreased CBF. We therefore compared CBV, CBF, and mean cortical thickness measured using MRI in a group of healthy controls, patients with MCI who converted to dementia due to AD (MCI-c), and patients with AD and mild dementia.

5.3 Participants

The study sample comprised patients with MCI that converted to dementia due to AD (MCI-c) (n=16), patients with mild Alzheimer's dementia (n=12) and control subjects (n=20). Demographic and cognitive data are shown in Table 5.1. The demographic and clinical data of the participants are shown in Table 5.1. No significant differences between groups were found for any of the variables studied, except in the MMSE score, which was lower in the AD and MCI converter groups than in the control group (p<0.0001).

Table 5.1: Demographic and clinical data of the participants.

	Controls, n=20	MCI-c, n=16	Alzheimer, n=12
Age in years (SD)	71.65 (7.04)	72.94 (6.53)	77.42 (6.97)
Sex (F:M)	11:9	11:5	4:8
Years of education (SD)	9.1 (4.36)	6.56 (2.90)	7.08 (5.38)
MMSE (SD) [a]	27.55 (2.09)	21.75 (4.40)[b]	19.08 (3.15)[b]
CDR	0	0.5	1

CDR=Clinical Dementia Rating; MCI-c: mild cognitive impairment converters; MMSE=Mini-Mental State Examination. [a](p<0.0001) ANOVA of group differences. [b] Significant differences (p<0.0001) with the control group in the post hoc Dunnett's test.

5.4 Statistical analysis

Differences in demographic and clinical data were tested using an ANOVA model.

Group differences in whole-brain cortical GM volume were tested using an ANCOVA model with age as a covariate. Lobar differences were tested using the same ANCOVA model, in order to determine which lobes contributed most to the reduction in cortical volume. Another ANCOVA model including age and whole-brain cortical GM volume as covariates was used to test for differences in mean cortical thickness and hippocampi and amygdalae volumes between the three groups (controls, MCI-c, and AD). The adjusted values for mean cortical thickness provide us with information about which regions are more deeply affected by the disease in the frame of global atrophy.

In order to test for regional differences in CBV and CBF mean values, we used an ANOVA model, since no effects of age or whole-brain cortical GM volume were observed in perfusion values.

Whenever the ANCOVA or ANOVA model revealed significant differences between groups, we used a post hoc procedure (Dunnett's test) to compare means between each patient group and controls. In variables showing significant differences between group means, the effect size (Cohen's coefficient, d) was calculated to assess the magnitude of those differences. The correlation between cortical thickness and perfusion variables (CBF, CBV) was studied using Pearson's correlation. Data were analyzed using Statistical Analysis System (SAS) version 9.0 (SAS Institute Inc., Cary, North Carolina, USA).

5.5 Results

5.5.1 Structural measurements

Considering the age effect in the ANCOVA, AD and MCI-c patients had smaller global cortical volumes than controls. Dunnett's test showed that those differences were more significant in MCI ($p<0.01$) than in AD ($p<0.05$). In a lobe-based analysis, ANCOVA revealed significant differences in the frontal lobes ($p<0.05$), right cingulated cortex ($p<0.05$), parietal lobes ($p<0.01$), and temporal lobes in their lateral ($p<0.01$) and medial aspect ($p<0.01$). Only the occipital lobes did not play a role in global cortical atrophy.

ANCOVA for the adjusted values of the mean cortical thickness was only significant in the medial temporal lobes ($p<0.01$) and posterior cingulated cortex ($p<0.05$). However, when each gyrus was analyzed independently, cortical thinning was detected in some of the gyri in the parietal and frontal lobes in the patient groups. Table 2 shows the effect size and statistical significance (Dunnett's test) for gyrus-based ROI differences. Both patient groups also had lower GM volumes in the hippocampi and amygdalae after adjustment for age and global cortical volume (table 3). Although MCI-c patients had more widespread atrophy than AD patients, the atrophy in the latter group was clearly more pronounced in the left pars triangularis, bilateral entorhinal cortex, left amygdala, and left hippocampus (Table 5.2 and Table 5.3).

Table 5.2: Cohen's coefficient/Dunnett's test p value for between-group differences.

Cortical regions	Hemisphere	Cortical Thickness		CBF		CBV	
		Controls-MCI-c	Controls-AD	Controls-MCI-c	Controls-AD	Controls-MCI-c	Controls-AD
Frontal							
Pars triangularis	Left	-0.95/0.021	-1.73/0.002	-	-	-	-
Pars opercularis	Left	-	-		-1.29/0.005	-	-
Pars orbitalis	Right	-	-		-	-	0.80/0.035
Paracentral	Left	-1.39/0.004	-		-	-	-
	Right	-	-	-0.81/0.022	-	-	-
Precentral	Right	-1.42/0.008	-	-	-	-	-
Rostral middle	Left	-	-	-	-1.48/0.002	-	-
	Right	-	-	-	-1.11/0.006	-	-
Parietal							
Superior gyrus	Left	-	-	-1.21/0.003	-	-	-
	Right	-	-	-0.88/0.021	-	-	-
Supramarginal	Left	-	-	-	-1.25/0.003	-	-
Precuneus	Left	-1.32/0.011	-	-	-	-	-
	Right	-1.26/0.014	-	-0.84/0.031	-	-	-
Temporal (lateral)							
Superior gyrus	Left	-	-	-	-1.44/<0.001	-	-1.23/0.003
	Right	-	-	-	-1.10/0.016	-	-
Banks	Left	-	-	-	-1.19/0.004	-	-0.78/0.020
Middle gyrus	Left	-	-	-	-1.17/0.004	-	-
Temporal (medial)							
Entorhinal cortex	Left	-1.35/0.001	-2.49/<0.0001	-	-	-	-
Entorhinal cortex	Right	-1.31/0.005	-2.02/<0.001	-	-	-	-
Parahippocampal gyrus	Right	-1.03/0.008	-1.35/0.016	0.98/0.021	0.84/0.040	-	0.85/0.023
Fusiform gyrus	Right	-	-	-	1.55/<0.001	-	-
Posterior Cingulate							
Isthmus division	Right	-	-1.26/0.014	-	-	-	-
Occipital							
Lingual gyrus	Left	-	-	-	0.89/0.032	-	-0.94/<0.01

CBF, cerebral blood flow; CBV, cerebral blood volume; MCI-c, mild cognitive impairment converters; AD, Alzheimer's disease. Negative coefficient=control values greater than patient values; positive coefficient=control values less than patient values.

Table 5.3: Cohen's coefficient/Dunnett's test p value for between-group differences.

Subcortical regions	Hemisphere	Grey matter volume		CBF		CBV	
		Controls-MCI-c	Controls-AD	Controls-MCI-c	Controls-AD	Controls-MCI-c	Controls-AD
Hippocampus	Left	-1.48/0.026	-1.98/<0.001	-	-	-	-
	Right	-1.80/0.006	-1.67/0.010	-	-	-	-
Amygdale	Left	-1.56/0.003	-1.81/0.001	-	-	-	-
	Right	-1.46/0.005	-1.31/0.035	-	-	-	-

CBF, cerebral blood flow; CBV, cerebral blood volume; MCI-c, mild cognitive impairment converters; AD, Alzheimer's disease. Negative coefficient=control values greater than patient values.

5.5.2 Cerebral blood volume and cerebral blood flow data

We did not observe statistically significant differences between patients and controls for mean CBV or CBF values in the whole brain cortex. For regional CBV data, ANOVA revealed statistical differences in the left occipital lobe ($p<0.05$) and left lateral temporal lobe ($p<0.01$), with lower mean values in the AD group than in the controls. No significant differences were found for CBV data in the MCI-c group. For regional CBF data, ANOVA revealed statistical differences between groups in the parietal lobes ($p<0.05$), left lateral temporal lobe ($p<0.05$), and right medial temporal lobe ($p<0.05$), where these differences revealed a hyperperfusion pattern: both patient groups had higher mean values than controls. Dunnett's post-hoc analysis revealed perfusion differences (only in CBF) in the MCI-c group in the parietal and temporal lobes; perfusion differences (CBV or CBF) in the AD group were also detected in the frontal and occipital lobes (Figure 5.1 and Figure 5.2). Table 5.2 shows the effect size and statistical significance based on Dunnett's test for gyrus-based ROI differences.

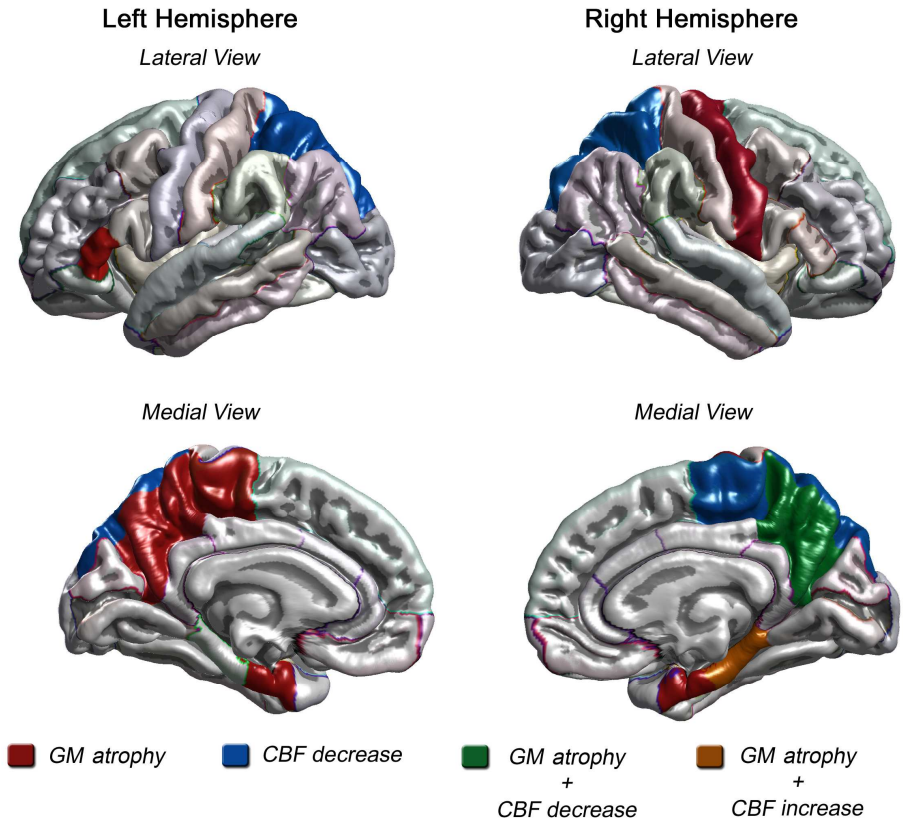

Figure 5.1: Representation of regions of interest (ROIs) showing significant differences in the post hoc test (Dunnett) between patients with mild cognitive impairment and controls. p value of Dunnett's test and effect size of the differences in represented ROIs are shown in Table 5.2. CBF, cerebral blood flow; CBV, cerebral blood volume; GM, gray matter.

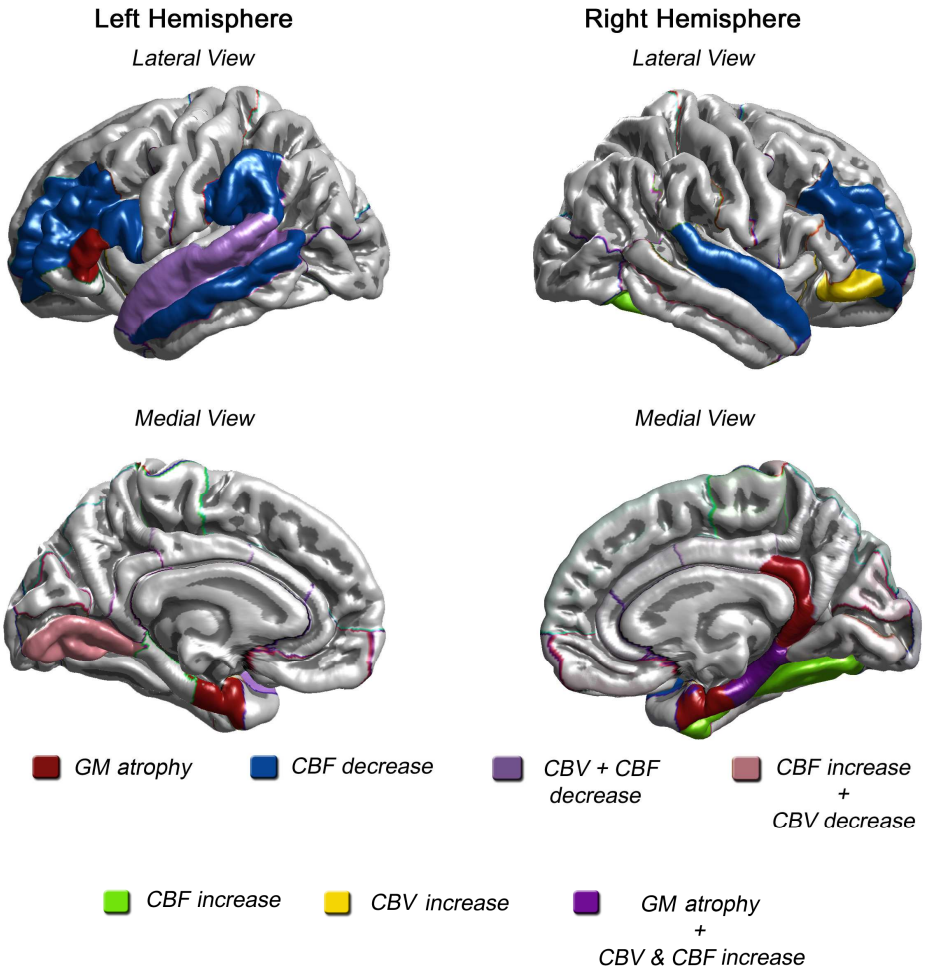

Figure 5.2: Representation of regions of interest (ROIs) showing significant differences in the post hoc test (Dunnett) between patients with Alzheimer's disease and controls. p value of Dunnett's test and effect size of the differences in represented ROIs are shown in Table 5.2. CBF, cerebral blood flow; CBV, cerebral blood volume; GM, gray matter.

5.5.3 Correspondence between perfusion values and atrophy

In the MCI-c group, CBF abnormalities coincided with a reduction in cortical thickness only in the right precuneus and right parahippocampal gyrus (Figure 5.1). The correlation between CBF data and the mean cortical thickness in the right precuneus was not significant, regardless of whether we used raw values for mean cortical thickness or

adjusted values after correcting for age and whole brain cortical GM volume. However, a significant negative correlation was detected between CBF and adjusted values of mean cortical thickness in the right parahippocampal gyrus ($r = -0.61$; $p=0.012$).

In AD, an increase in CBV and CBF coincided with cortical thinning in the right parahippocampal gyrus (Figure 5.2), although no correlation was found between variables with raw or adjusted values for cortical thickness.

5.6 Discussion

Cortical thinning in the initial stages of AD does not necessarily match hypoperfused brain regions, thus reinforcing the contribution of perfusion MRI as independent variable in the characterization of AD (Figure 5.1 and Figure 5.2). Our study suggests that CBF deficits appear before CBV deficits in the progression of AD, since CBV abnormalities were only detected at the stage of AD, whereas CBF changes were already detected in the MCI stage. Therefore, our results confirm the hypothesis that CBF is a more sensitive parameter than CBV for perfusion abnormalities in patients with MCI. CBF could reflect neuronal dysfunction, whereas CBV could reflect changes in microvasculature architecture as a consequence of prolonged neuronal dysfunction (Bell and Ball, 1981).

5.6.1 Structural measurements

The analysis by lobar ROIs showed a characteristic pattern of atrophy in early AD, which was previously described in the literature using the same brain parcellation method (McDonald et al., 2012). The medial temporal lobes and posterior cingulated cortex seem to present higher atrophy in early stages of disease, since significant differences between groups persisted after correcting for global cortical atrophy. Changes in the posterior cingulate cortex could be closely related to those in the entorhinal cortex in patients with AD (Hirao et al., 2006). Atrophy in the AD group was more pronounced than in the MCI-c group in the entorhinal cortex, left hippocampus, left amygdala, and left pars triangularis. This observation could be explained by longer disease duration or stronger tissue involvement in AD than in MCI-c.

5.6.2 Perfusion measurements

A significant decrease in CBF in parietal lobes was detected in the MCI-c group, although no significant changes in CBV were detected in this group. Were it confirmed that hypoperfusion in the parietal lobes is a predictor for rapid conversion from MCI to AD (Hirao et al., 2005), our results would suggest that CBF could be a more useful biomarker than CBV for progression of MCI to AD. A reduction in capillary diameter in response to neuronal deactivation could have a greater effect on CBF values than on CBV, probably because of the Hagen-Poiseuille equation, according to which flow in a tube (vessel) of a radius R changes with a factor R^4, whereas the corresponding volume of the tube changes with a factor R^2. Therefore, cerebral changes would imply a relatively greater change in flow than in volume (Kolbitsch et al., 2000). Prolonged neuronal deactivation or the spread of AD neuropathology across the brain could have a more intense effect on microvasculature architecture (capillary density), thus increasing CBV differences in more advanced stages of AD (Kitaguchi et al., 2007). CBV could be more related to tissue atrophy (Uh et al., 2009).

A hyperperfusion pattern was detected in the medial temporal lobes in both patient groups, suggesting the existence of compensatory mechanisms (Dai et al., 2009; Dickerson and Sperling, 2008). In the MCI-c group, this hyperperfusion was detected as an increase in CBF, while in AD it was also detected as an increase in CBV. The increase in CBV in the AD group could represent changes in the microvasculature architecture. On neural activation, astrocytes not only regulate capillary diameters (Koehler et al., 2009) but they also stimulate the mitogenic activity of capillary endothelial cells, suggesting that prolonged functional hyperemia may initiate angiogenesis, which could result in increased capillary density (Harder et al., 2002). This observation could explain the findings of Bell and Ball (Bell and Ball, 1981), who detected areas of the medial temporal lobes with higher levels of capillary density in the brains of AD patients than in the brains of controls. In those areas, capillary density correlated positively with neuronal degeneration. Hyperperfusion has also been attributed to inflammatory processes (Alsop et al., 2008). Inflammation studies in AD have reported activated microglia surrounding β-amyloid deposits within the brain, which may be responsible for a locally induced

chronic inflammatory response (Salminen et al., 2009; Wilkinson et al., 2012). Inflammation could explain the increase in capillary density in those areas with upregulated inflammatory responses (Fiedler and Augustin, 2006; Jackson et al., 1997).

5.6.3 Correspondence between perfusion values and atrophy in patients

Although the MCI-c group presented more widespread atrophy than AD patients, the AD group showed more hypoperfused regions than the MCI-c group. These findings could support the idea that atrophy does not explain cognitive deficits *per se* and that vascular factors play a key role in the decline of cognition in AD (Henry-Feugeas, 2008); therefore, treatments which stabilize or increase brain perfusion could delay cognitive deterioration or even improve cognitive functions (Van Beek and Claassen, 2011; Mueller et al., 2006; Nakano et al., 2001). In MCI-c, a negative correlation between CBF values and cortical thickness in the right parahippocampal gyrus suggests an increase in CBF that is dependent on cortical atrophy. In AD, this correlation disappears, suggesting a breakdown of compensatory mechanisms (Clement and Belleville, 2010) or a reduction in inflammatory processes in more advanced stages of the disease. Future studies in this field could elucidate the etiology of hyperperfusion in pre-dementia and early stages of AD.

Our study is subject to a series of limitations. Statistical power is limited by the reduced sample size, and differences in spatial resolution between T1 and PI studies may cause tissue registration mismatch; therefore, errors in the cortical parcellation of CBF and CBV maps cannot be controlled. The most important limitation of this study is that we performed a cross-sectional comparison of two groups of patients in different clinical situations instead of a longitudinal study. Longitudinal mapping of perfusion parameters could prove more interesting for the characterization of perfusion abnormalities during progression of AD. The main asset of our study is the multimodal nature of the data (T1 and PI), which allowed us to apply an easily reproducible method for cortical parcellation, by incorporating structural information in the perfusion data. In addition, our access to information on the clinical progression of MCI-c enabled us to obtain the

greater value of CBF compared with CBV as a perfusion deficit biomarker in a group of MCI patients who converted to dementia due to AD.

5.7 Conclusions

In summary, in the MCI converter group we observed a significant decrease in CBF in the parietal lobes and a significant increase in CBF in the right medial temporal lobe. The negative correlation between CBF values and cortical thickness in the right parahippocampal gyrus suggested an increase in CBF that was dependent on cortical atrophy in pre-dementia stages of AD. Since perfusion deficits were detected in CBF and not in CBV, our results suggest that CBF maps can better characterize perfusion abnormalities in pre-dementia stages of AD than CBV.

6 THE DISCONNECTION HYPOTHESIS IN ALZHEIMER'S DISEASE STUDIED THROUGH MULTIMODAL MRI: STRUCTURAL, PERFUSION AND DIFFUSION TENSOR IMAGING

This chapter has been submitted as original article: Brain

6.1 Abstract

According to the so-called disconnection hypothesis, the loss of synaptic inputs from the medial temporal lobes in Alzheimer's disease (AD) may lead to reduced activity of target neurons in allocortical areas and, consequently, to decreased cortical blood perfusion in those areas. The aim of this study was to assess whether hypoperfusion in the parietotemporal and frontal cortices of patients with early AD is associated with atrophy in the medial temporal lobes and/or microstructural changes in the white matter (WM) tracts connecting these areas. We also studied the relationship between cortical atrophy in the medial temporal lobe and microstructural changes in the WM tracts of the limbic system. We assessed these relationships by investigating correlations between cerebral blood flow (CBF) in hypoperfused areas, mean cortical thickness in atrophied regions of the medial temporal lobes, and fractional anisotropy (FA) in WM tracts. These correlations were computed in a group of 16 patients with mild cognitive impairment who subsequently converted to dementia due to AD (MCI-c) and 12 patients with mild AD. We did not find a correlation between CBF deficits in the parietotemporal and frontal cortices and cortical thinning in the medial temporal lobes in either the MCI-c or the AD group. In the MCI-c group, however, a strong correlation was observed between CBF of the superior parietal gyri and FA in the parahippocampal tracts (left: $r=0.90$, $p<0.0001$; right: $r=0.597$, $p= 0.024$), and between FA in the right parahippocampal tract and the right precuneus ($r=0.551$, $p=0.041$). These results support the hypothesis of disconnection syndrome. No significant correlations between CBF in hypoperfused regions and FA in the WM tract were observed in the AD group. Therefore, factors other

than disconnection syndrome may be involved in perfusion deficits in this group. We did not find correlations between cortical thinning in the medial temporal lobes and decreased FA in the WM tracts of the limbic system in either group.

6.2 Introduction

Cognitive functions seem to be the result of temporally coordinated neuronal activity in more than one brain region, integrated into neural networks, rather than activation of an isolated group of cells (Horwitz et al., 2005; McIntosh and Gonzalez-Lima, 1994). Disruption of these functional networks may lead to cognitive impairment. Several neuroimaging studies point to the existence of cortical disconnection as a possible cause of cognitive impairment in Alzheimer's disease (AD). According to this hypothesis, AD-related symptoms would be the consequence—at least partially—of abnormal interactions between neuronal systems, rather than the effect of localized pathophysiology in one or more brain regions (Bokde et al., 2009; Delbeuck et al., 2003). In fact, a strong correlation has been reported between synapse loss and cognitive impairment, whereas a weak correlation exists between clinical symptoms and the level of deposition of amyloid plaques and intracellular formation of tangles (Terry et al., 1991). The loss of synaptic inputs in cortical neurons may lead to a reduction in the activity of target neurons and, consequently, to a decrease in cerebral blood flow (CBF) in the corresponding cortical target area (A. D. Smith, 2002). According to this hypothesis, hypoperfusion in the parietotemporal and frontal cortices observed in the pre-dementia and mild dementia stages of AD in our previous work (Lacalle-Aurioles et al., 2014) might be related to a disconnection of these regions from the medial temporal lobe.

The combination of MRI techniques (structural, diffusion, and perfusion) could elucidate the structural and functional features of the disconnection hypothesis. Perfusion MRI is a good alternative to nuclear medicine for the evaluation of cerebral blood perfusion. It has the advantages of shorter acquisition time, lower cost, and no need for ionizing radiation, thus facilitating clinical routine and patient comfort. Diffusion tensor imaging (DTI) provides information about water diffusion properties in brain tissues at the cellular level. White matter (WM) tracts present higher diffusion anisotropy than other tissues. This anisotropy could be altered even in preclinical stages of AD. Fractional anisotropy (FA) is a DTI measurement (Basser and Pierpaoli, 1996) that indirectly quantifies the degree of geometric organization of axonal bundles across the brain (Beaulieu, 2002). DTI plays a

relevant role in the study of microstructural changes in WM fibers in the progression of AD (Medina and Gaviria, 2008; Zhang et al., 2014). Reduced fiber density or decreased myelination in fiber tracts manifests as decreased FA (Mori and Zhang, 2006).

All 3 MRI techniques have been combined for the characterization of patients with mild cognitive impairment (MCI) and AD (Zimny et al., 2011, 2013). However, these studies focused on the use of the three techniques in the same regions, namely, the posterior cingulate cortex and the hippocampus. To our knowledge, there are no previous reports on the relationships between atrophy of the cortical gray matter (GM) of the medial temporal lobe, perfusion deficits in parietotemporal and frontal cortices, and microstructural changes in the WM tracts connecting such structures. The aim of our work was to study possible correlations between CBF values in hypoperfused areas, mean cortical thickness in the medial temporal lobe, and FA in the WM tracts. We also studied the correlation between cortical atrophy in the medial temporal lobes and microstructural changes in the WM tracts of the limbic system. Linear correlations were computed separately in three groups: patients with MCI who converted to dementia due to AD, patients with mild AD dementia and healthy controls.

6.3 Participants

Forty-eight subjects were included in the study and classified into three groups: subjects with mild cognitive impairment who converted to dementia due to AD after two years of clinical follow-up (MCI-c) (n=16), patients with AD and mild dementia (n=12), and volunteers with normal cognition (n=20). MRI-based structural and perfusion data were obtained from all participants. Diffusion data could only be obtained from 16/20 controls, 14/16 MCI-c and 10/12 AD due to patient movements during the image acquisition. The Table 6.1 summarizes demographic and clinical data of the participants who undergone DTI scan. No significant between-group differences were found for these demographic variables, except for the Mini-Mental State Examination (MMSE) score, which was lower in the AD and MCI-c groups than in the control group.

Table 6.1: Demographic and clinical data of the participants included in the between-group comparative analysis for patients who had a DTI scan.

	Controls n=16	MCI-c n=14	Alzheimer n=10
Age in years (SD)	71.25 (6.71)	73.43 (6.20)	76.80 (7.36)
Sex (Female:Male)	10:6	9:5	3:7
Years of education (SD)	9.69 (4.41)	7.14 (2.60)	8.00 (5.42)
MMSE (SD) ***	27.38 (2.19)	21.36 (4.55) [a]	19.40 (3.17) [a]
CDR	0	0.5	1

MCI-c: mild cognitive impairment converters to AD. ***($p<0.0001$) ANOVA of group differences. a Significant differences ($p<0.0001$) with the control group in the post hoc Dunnett's test. MMSE=Mini-Mental State Examination; CDR=Clinical Dementia Rating.

6.4 Quantification

The first step in our study was to detect which WM tracts of the whole brain presented microstructural changes in each patient group. We then performed a correlation analysis focusing on the altered WM tracts that presumably connect atrophied areas of the medial temporal lobe with hypoperfused regions in the parietotemporal and frontal cortices. Gyrus-based ROIs which showed cortical thinning and hypoperfusion were taken from a previous work that studied the same sample (Lacalle-Aurioles et al., 2014).

We finally selected significantly altered WM tracts of the limbic system to study correlations between microstructural changes in WM tracts and atrophy of the medial temporal lobe.

Tract-based ROIs analysis and selection

We carried out a between-group comparative analysis of FA values in WM tracts of the whole brain in order to detect possible microstructural changes in WM fibers between the study groups. We compared mean FA values of tract-based ROIs in the major association fibers and limbic system fibers from both hemispheres and callosal tracts (Wakana et al., 2004). In the case of the association fibers, we focused on the superior longitudinal fasciculus, the superior fronto-occipital fasciculus (which connects the frontal, temporal, parietal, and occipital lobes) and the uncinate fasciculus (which connects the temporal

and frontal lobes). In the case of the limbic system tracts, we focused on the cingulum, fornix, fornix-stria terminalis (ST), and the parahippocampal tract (i.e., the part of the cingulum situated in the medial temporal lobe). Callosal tracts included the genu, the body, and the splenium.

Correlation analysis of CBF, mean cortical thickness and FA data

Figure 6.1 illustrates the set of ROIs included in the correlation analysis in each patient group. In the control group, correlations were computed for the same ROIs selected in both patient groups.

In order to unveil possible associations between perfusion deficits in the parietotemporal and frontal cortices and atrophy in the medial temporal lobes, we investigated correlations between the mean cortical thickness of the atrophied ROIs and CBF values of the hypoperfused ROIs in each hemisphere. We also investigated correlations between CBF in hypoperfused ROIs and the FA data of the cingulate and parahippocampal WM tracts that revealed significant microstructural differences in the comparative analysis of WM tracts. These two specific tracts were selected because they connect the medial temporal lobe with the parietal, frontal, and lateral temporal lobes (Bokde et al., 2009).

Finally, we correlated the mean cortical thickness in atrophied ROIs of the medial temporal lobe with FA values of WM tracts of the limbic system that showed significant microstructural changes in the previous comparative analysis.

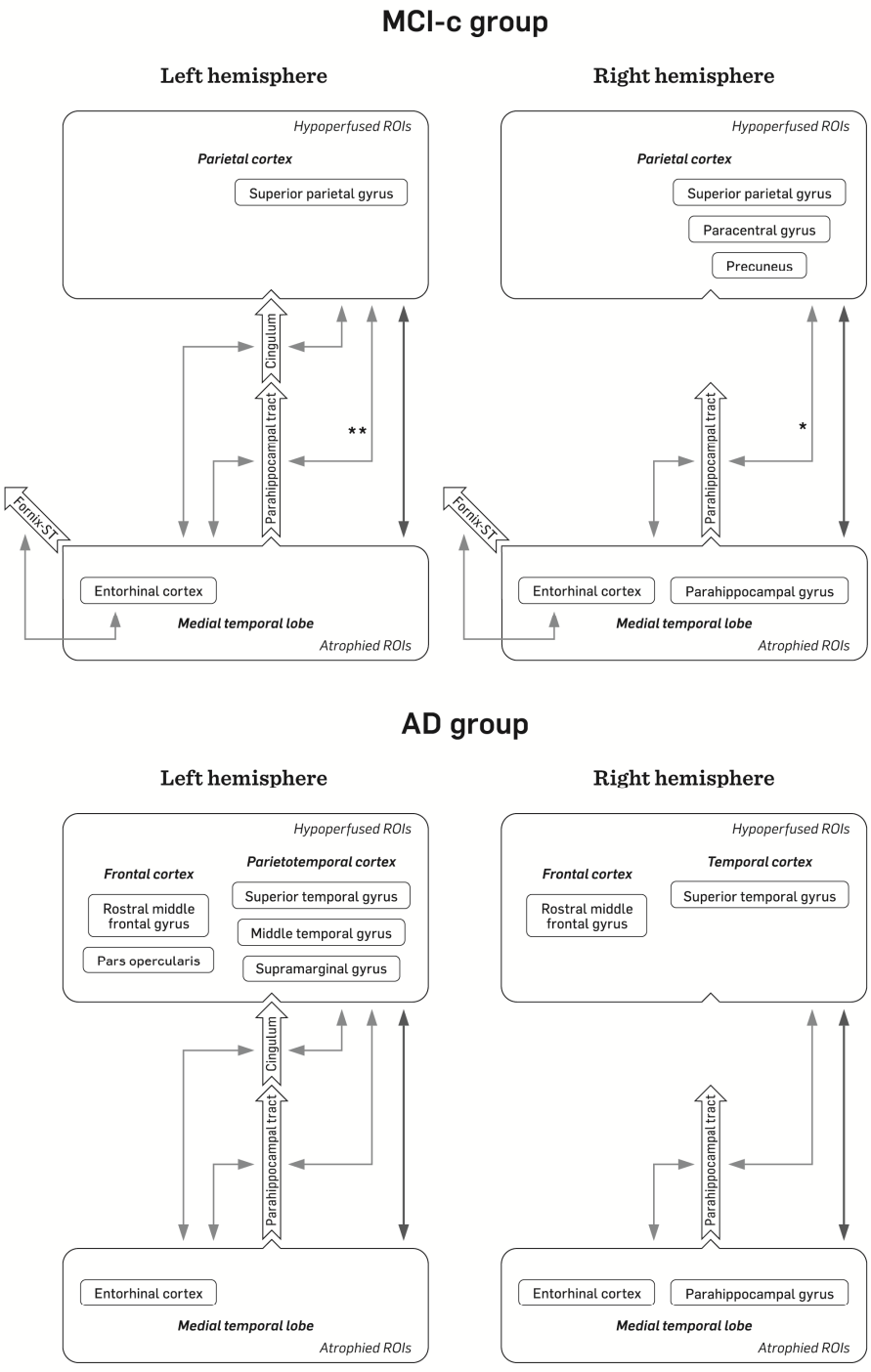
MCI-c group
Left hemisphere
Right hemisphere
Hypoperfused ROIs
Parietal cortex
Superior parietal gyrus
Paracentral gyrus
Precuneus
Cingulum
Parahippocampal tract
Fornix-ST
**
*
Entorhinal cortex
Parahippocampal gyrus
Medial temporal lobe
Atrophied ROIs
AD group
Left hemisphere
Right hemisphere
Hypoperfused ROIs
Frontal cortex
Parietotemporal cortex
Temporal cortex
Rostral middle frontal gyrus
Pars opercularis
Superior temporal gyrus
Middle temporal gyrus
Supramarginal gyrus
Cingulum
Parahippocampal tract
Entorhinal cortex
Parahippocampal gyrus
Medial temporal lobe
Atrophied ROIs

Figure 6.1: Diagram of the correlations computed between mean cortical thickness in atrophied areas, cerebral blood flow in hypoperfused areas, and fractional anisotropy in white matter tracts in selected regions of interest (ROIs) for each patient group. Wide arrows correspond to tract-based ROIs that showed significant microstructural changes in the comparative analysis of WM tracts (see quantification section in Material and Methods). Two headed arrows indicate correlations between atrophied and hypoperfused gyrus-based ROIs, and between gyrus-based ROIs and tract-based ROIs. Asterisks indicate significant correlations: ** $p<0.0001$, * $p<0.05$.

6.5 Statistical analysis

We tested for between-group differences in FA in tract-based ROIs using an ANCOVA model including age as a covariate. Sex was not included in the model because we did not find any significant effect of this cofactor. When the ANCOVA model revealed significant differences between groups, we used a post hoc test (Dunnett's test) to compare mean values between patient groups and controls and computed the effect size (Cohen's coefficient, d). We used Pearson's coefficient to study correlations. Data were processed using Statistical Analysis System (SAS) version 9.0 (SAS Institute Inc., Cary, North Carolina, USA).

6.6 Results

6.6.1 Comparative ROI-based analysis of FA data

The ANCOVA model revealed significant between-group differences in the genu ($p=0.025$), splenium ($p=0.035$), left cingulate tract ($p=0.014$), parahippocampal tracts (left: $p=0.003$; right: $p=0.001$), and fornix-ST (left: $p=0.027$; right: $p=0.003$). Figure 6.2 shows tract-based ROIs which presented significant FA differences between each patient group and controls. Table 6.2 summarizes the effect size and p value (Dunnett's test) for differences in FA between controls and each patient group.

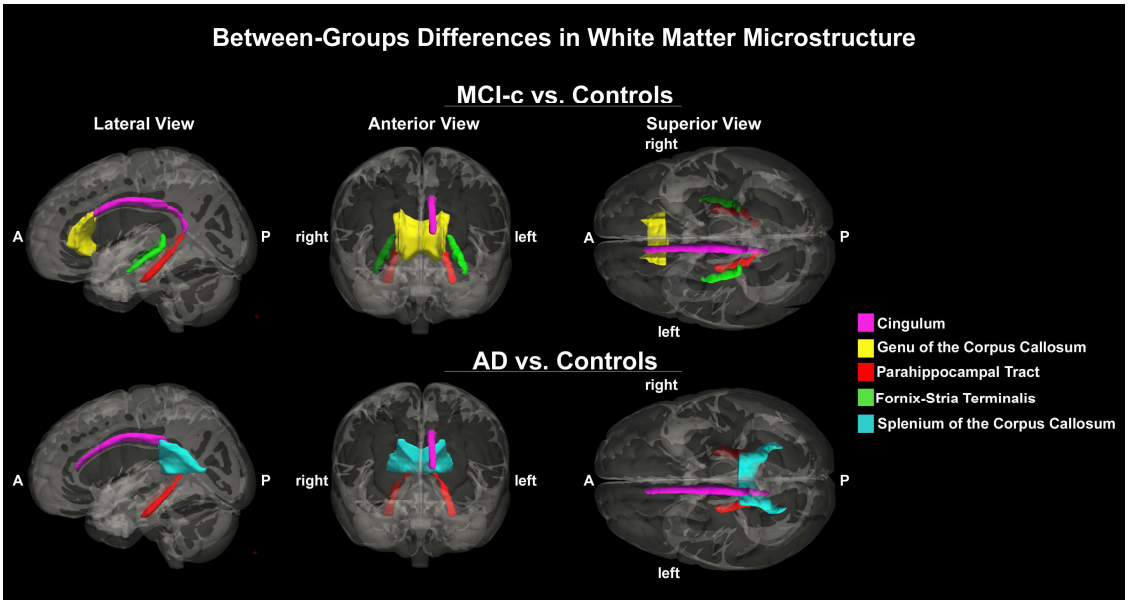

Figure 6.2: Tract-based ROIs showing significant differences between patient groups and controls.

Table 6.2: Tract-based ROI analysis of fractional anisotropy (FA). FA measurements are indicated as mean (SD). Differences between controls and patients groups are assessed by Cohen's d coefficients and Dunnett's test p values.

Location	Control n=16	MCI-c n=14	AD n=10	control vs MCI-c	control vs AD
	Mean (SD)	Mean (SD)	Mean (SD)	d / p	d / p
Genu	0.528 (0.033)	0.496 (0.030)	0.490 (0.034)	-1,01/0.023	-
Splenium	0.612 (0.029)	0.590 (0.033)	0.570 (0.031)	-	-1,41 /0.024
Cingulum (L)	0.439 (0.023)	0.414 (0.021)	0.413 (0.022)	-1,13/0.014	-1,15 /0.044
Fornix-ST (L)	0.484 (0.029)	0.453 (0.029)	0.466 (0.027)	-1,07/0.015	-
Fornix-ST (R)	0.452 (0.038)	0.403 (0.034)	0.421 (0.033)	-1,35/0.002	-
Parahippocampal tract (L)	0.413 (0.027)	0.367 (0.044)	0.360 (0.035)	-1,28/0.004	-1,75 /0.010
Parahippocampal tract (R)	0.412 (0.028)	0.361 (0.037)	0.366 (0.041)	-1,57/0.001	-1,37 /0.010

AD:Alzheimer's disease, MCI-c:mild cognitive impairment converters to AD, SD:standard deviation, (-):non-significant results. Negative value for Cohen's d coefficient: FA in patients<controls

6.6.2 Correlation between cortical thickness in the medial temporal lobe and CBF in parietotemporal and frontal cortices

We did not find a significant correlation between mean cortical thickness in the atrophied ROIs and CBF values in hypoperfused ROIs for any of the three groups studied.

6.6.3 Correlation between FA in the parahippocampal and cingulate WM tracts and CBF in parietotemporal and frontal cortices

A strong correlation between FA in the left parahippocampal tract and CBF of the left superior parietal gyrus was observed in the MCI-c group ($r=0.90$, $p<0.0001$). Correlations were found in the right hemisphere between FA in the parahippocampal tract and CBF of the superior parietal gyrus ($r=0.597$, $p= 0.024$) and precuneus ($r=0.551$, $p=0.041$) (Figure 6.3). No significant correlations were found for AD patients and controls.

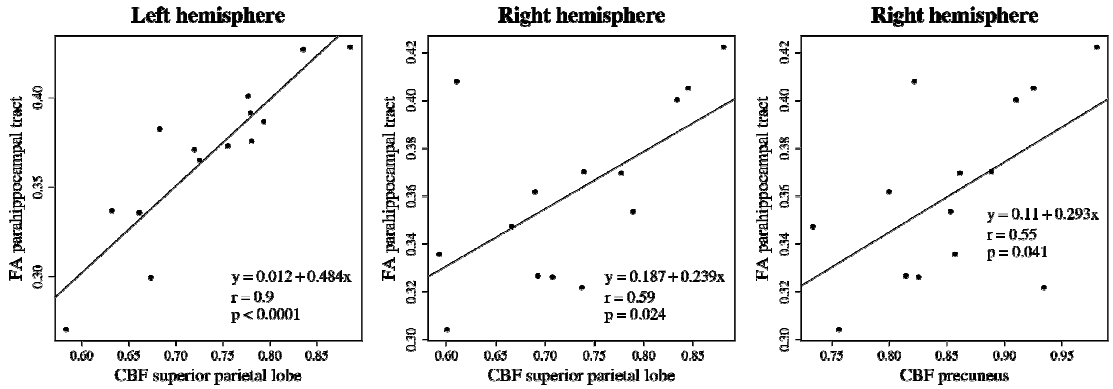

Figure 6.3: Scatter plots for significant correlation between fractional anisotropy in the hippocampal WM tracts and cerebral blood flow in hypoperfused parietal regions in the MCI-c group.

6.6.4 Correlation between cortical thickness in the medial temporal lobes and FA in WM tracts of the limbic system

We did not find a significant correlation between mean cortical thickness in atrophied ROIs and decreased FA in the tract-based ROIs studied for any of the three groups.

6.7 Discussion

According to the so-called disconnection hypothesis, perfusion deficit in the parietotemporal and frontal cortices of patients with AD is thought to be related to a functional disconnection from the medial temporal lobe. However, several

neuropathological studies have demonstrated that cerebrovascular lesions are very frequent in AD, making mixed dementia (neuronal and vascular) the most common type of dementia, especially in the later stages of the disease (Henry-Feugeas, 2009; Korczyn and Vakhapova, 2007). The study of hemodynamic alterations using multimodal MRI may help to elucidate whether perfusion deficits in AD patients are related to disconnection syndrome or not.

In the present study we investigated possible correlations between cortical atrophy in the medial temporal lobes, CBF deficits in the parietotemporal and frontal cortices, and decreased FA in WM tracts connecting these areas. To our knowledge, this is the first study to apply multimodal MRI (structural, perfusion, and diffusion) to test the disconnection hypothesis by comparing patients with AD, MCI-c, and aged-matched healthy controls. According to our results, in the MCI-c group, hypoperfusion in the parietal lobes is related to a decrease in FA in parahippocampal WM fibers but not to cortical thinning in the medial temporal lobe. In the AD group, the lack of a correlation between CBF in the parietotemporal and frontal cortices and FA in WM tracts (or cortical thickness in the medial temporal lobe) suggests that widespread perfusion deficits in this group are not associated with disconnection syndrome, thus supporting studies that propose a mixed etiology (neuronal and vascular) for AD (Altman and Rutledge, 2010; Bell, 2012).

6.7.1 Between-group comparative analysis for FA data

Our results in the comparative tract-based ROI analysis agree with previously published data. Decreased FA in the cingulate and parahippocampal WM tracts, fornix, and corpus callosum has been extensively reported in MCI and AD patients in the literature (Fellgiebel et al., 2008; Mielke et al., 2009; Rose et al., 2000, 2006; Teipel et al., 2007; Zhang et al., 2007). Possible damage to these WM tracts could underlie the breakdown of functional networks that could in turn generate cognitive impairment. The hippocampus, cingulum, and fornix axis form part of the memory circuit, and microstructural changes in those tracts are considered potential imaging markers of brain changes in preclinical stages of AD (Zhang et al., 2014). Microstructural changes in the parahippocampal WM

fibers could indicate degeneration of the connections between the medial temporal lobes and allocortical areas. Changes in the fornix-ST may correspond to damaged connections between the entorhinal cortex, amygdala, and the mammillary bodies, which are implicated in memory tasks. Some authors have observed a strong correlation between FA values in the fornix and performance in episodic memory tests in patients with MCI and AD, suggesting that damage in this structure is an early marker of progression of AD (Mielke et al., 2009). Changes in cingulate WM fibers could affect connectivity between the anterior thalamus, cingulate cortex, association cortices (in the frontal, temporal, and parietal lobes), and the hippocampi (Bokde et al., 2009). The decreased FA observed in some regions of the corpus callosum in the MCI-c group (genu) and the AD group (splenium) could indicate the occurrence of interhemispheric disconnection early in AD (Rose et al., 2000).

6.7.2 Correlations between atrophy in the medial temporal lobes, microstructural changes in parahippocampal WM fibers and hypoperfusion in parietotemporal and frontal cortices in early Alzheimer's disease.

The existence of atrophy of the medial temporal lobes and reduced blood perfusion in the parietotemporal lobes of patients with AD was described by Jobst et al. (Jobst et al., 1992), who also reported that the asymmetrical severity of atrophy of the medial temporal lobes was matched by an asymmetrical reduction in CBF in the parietotemporal regions. These results agree with the idea that the loss of neuronal inputs from the hippocampal region may play a role in the decrease in CBF in functionally connected cortical areas. As we reported in our previous work (Lacalle-Aurioles et al., 2014), atrophy in MCI-c patients was more extensive in the right medial temporal lobe than in the left one, and larger hypoperfused areas were also observed in the right parietal lobe, consistent with the observations of Jobst et al. However, in the present study, we did not find a correlation between cortical thinning in the atrophied medial temporal lobes and CBF values in any of the hypoperfused ROIs in the parietal lobes. This result suggests that the degree of parietal hypoperfusion is not directly related to the level of atrophy in the medial temporal lobes.

On the contrary, the fact that CBF values in parietal lobes correlate with FA values in the parahippocampal WM tracts suggests that hypoperfusion in the parietal lobes is related to microstructural changes in WM fibers, which connect hypoperfused areas with the medial temporal lobes. This observation is consistent with the idea that reduced activity in the parietotemporal and frontal cortices may be associated with damage in neuronal connections instead of with macrostructural changes in the cortex of the medial temporal lobes. The parietal lobe has traditionally been associated with spatial attention and visuo-motor control (Malhotra et al., 2009). However, functional MRI studies have defined a parieto-hippocampal network associated with memory tasks (Vincent et al., 2006). Our results suggest that, owing to microstructural alterations in WM fibers connecting both lobes, this network could be physically damaged in the MCI-c patients we assessed. The results observed in the MCI-c group could support the existence of a disconnection syndrome that already appears in pre-dementia stages. To our knowledge, the present study is the first to use multimodal MRI to show evidence of disconnection syndrome that is potentially unrelated to cortical atrophy in MCI-c patients.

In AD patients, hypoperfusion in the parietotemporal and frontal areas seemed to be unrelated to either cortical thinning in the medial temporal lobes or microstructural changes in the WM fibers in the parahippocampal and cingulate tracts, suggesting that hemodynamic alterations in this group may not be related to a disconnection effect. Other vascular factors such as amyloid deposition around blood vessels may lead to blood perfusion deficits. These vascular alterations are associated with the accumulation of neurotoxic molecules in the cerebral cortex that may subsequently contribute to neuronal degeneration (Zlokovic, 2011). However, since the lack of significant correlations could be due to the small sample size, results are not decisive in this group.

On the other hand, in both MCI-c and AD patients, decreases in FA in the parahippocampal and left cingulate tracts did not correlate with thinning of the cortex in the parahippocampal gyrus and the entorhinal cortices. Similarly, in MCI-c, the FA of the fornix-ST did not correlate with entorhinal cortical thickness; these results suggest that reductions in FA are not associated with cortical atrophy in the medial temporal lobes, thus supporting that microstructural changes in WM are independent from

macrostructural cortical changes in the medial temporal lobes. This independence of macrostructural and microstructural changes was recently reported by Canu et al. and Palesi et al. in patients with mild to moderate AD (Canu et al., 2010; Palesi et al., 2012). However, a study in MCI patients proposed the existence of a sequence of events in which hippocampal atrophy induces a progressive breakdown of WM fibers, which could in turn lead to hypometabolism in other cortical areas (Villain et al., 2010). The authors demonstrated that correlation between hippocampal and WM atrophy was not present at baseline but existed between basal values in hippocampal atrophy and rate of changes in WM volume over time. Unfortunately, the authors only measured macrostructural changes in WM, since they used structural MRI instead of DTI; therefore, their findings are not comparable to ours.

The disconnection hypothesis is also supported by the results of histological studies: the distribution of AD-related neuropathology (neurofibrillary tangles and neuritic plaques) across the brain follows a vulnerability pattern that makes these markers particularly abundant in specific laminae in the cerebral cortex. Those specific laminae harbor pyramidal neurons responsible for cortico-cortical connections within and between hemispheres (Bokde et al., 2009). Therefore, an association seems to exist between cortical disconnection and the spread of the neuropathology and atrophy across the brain.

Although our sample size is similar to that of other DTI studies recently reviewed by Liu et al. (Liu et al., 2011) (each with 10 to 20 patients), the small number of participants limits statistical power. Therefore, our results should be interpreted with caution, especially for the AD group. Another limitation is the cross-sectional design. A longitudinal study could be more informative for the characterization and assessment of the progression of a possible disconnection syndrome. The main asset of our study is the multimodal nature of the data (T1, PWI, and DTI) used to test the hypothesis of a disconnection syndrome in early AD. In addition, our access to information on the clinical progression of the MCI group enabled us to test this hypothesis in prodromal AD (i.e., MCI-c group), according to the new lexicon for Alzheimer’s disease proposed by Dubois et al. (Dubois et al., 2010).

6.8 Conclusions

We did not find a correlation between CBF deficits in the parietotemporal and frontal cortices and cortical thinning in the medial temporal lobes in the MCI-c group or the AD group. Therefore, hypoperfusion seems not to be directly associated with medial temporal atrophy. In the MCI-c group, we observed a strong correlation between microstructural changes in the parahippocampal WM fibers and perfusion deficits in the parietal lobes: this finding may support the existence of a disconnection syndrome that could begin in pre-dementia stages of the disease. In the AD group, the lack of a correlation between CBF values in the parietotemporal and frontal cortices and FA in parahippocampal and cingulate WM fibers suggests that perfusion deficits in this group would not depend on disconnection syndrome. The lack of a correlation between mean cortical thickness in the medial temporal lobes and the FA in WM tracts of the limbic system in both groups suggests that microstructural changes in these tracts are not directly associated with cortical atrophy in the medial temporal lobes.

7 DISCUSIÓN

La detección de la EA en las fases anteriores a la demencia se ha convertido en un reto clínico y científico. Teniendo en cuenta que las terapias que se están desarrollando actualmente no son curativas y sólo pueden ralentizar el avance de la enfermedad (Ballard et al., 2007; Lyseng-Williamson and Plosker, 2002), conseguir un diagnóstico precoz que permita iniciar cuanto antes estas terapias mejoraría la calidad de vida de los pacientes y de sus familias, permitiéndoles prolongar la fase de la enfermedad donde aún conservan una mayor independencia. El empleo de la RM en la caracterización de los pacientes de EA permite encontrar cambios funcionales y estructurales en los tejidos cerebrales de los pacientes incluso en etapas preclínicas de la enfermedad, lo que la convierte en una herramienta muy valiosa para el diagnóstico precoz. Aunque la modalidad de RM más utilizada es la estructural, la RM de perfusión se ha incorporado recientemente a la rutina clínica con el fin de evaluar el estado de la vascularización cerebral de los pacientes, ya que se estima que el 80% de los pacientes padecen además alteraciones hemodinámicas asociadas a la EA (Henry-Feugeas, 2008). Este trabajo de tesis doctoral ha tenido como finalidad avanzar en la mejora de la detección, mediante RM de perfusión, de las alteraciones hemodinámicas que se producen en las fases más tempranas de la EA. Por otro lado, se pretendía conocer la relación existente entre dichas alteraciones hemodinámicas, la pérdida de SG cortical y el daño en las conexiones funcionales implicadas en tareas de memoria.

El objetivo de mejorar la detección de las alteraciones hemodinámicas se ha abordado, por un lado, mediante la búsqueda de una región de referencia para la normalización de los mapas paramétricos de perfusión que permitiese detectar el mayor número de regiones afectadas y, por otra parte, comprobando cuál de los parámetros de perfusión frecuentemente utilizados en los estudios de perfusión, CBV o CBF, era un biomarcador más temprano de las alteraciones hemodinámicas en los pacientes de EA.

Como se apuntaba en el capítulo de motivación, no se ha hecho hasta ahora ningún estudio de validación de una región de referencia para la normalización de intensidad de las imágenes de perfusión obtenidas con RM. En la literatura revisada se emplea

mayoritariamente el cerebelo, haciendo referencia a la validación de esta estructura en estudios de medicina nuclear (Bozzao et al., 2001; Harris et al., 1998; Uh et al., 2009). El proceso de normalización permite eliminar la variabilidad de intensidad debida a procesos biológicos y experimentales que dificultan la detección de las alteraciones hemodinámicas en los pacientes, por lo que resultaba importante confirmar si el cerebelo era también una región de referencia adecuada en estudios de RM. Tras haber comparado tres regiones de referencia (sustancia blanca total, cerebelo y sustancia gris cortical total), nuestros resultados nos permiten afirmar que, en el caso de los estudios de perfusión con RM, la sustancia gris cortical total permite la detección de un mayor número de regiones afectadas. Por lo tanto, parece ser una mejor región de referencia que el cerebelo para la normalización de mapas de perfusión en estudios de pacientes de Alzheimer en fases tempranas de la enfermedad.

Igualmente, tampoco se han encontrado en la literatura estudios comparativos sobre la sensibilidad de los parámetros de perfusión (CBV, CBF) a los cambios hemodinámicos en distintos estadios de la enfermedad. En esta tesis se hipotetizaba que el CBF sería más sensible en la detección de las anomalías hemodinámicas en las fases preclínicas de la enfermedad, puesto que este parámetro parece ser más sensible que el CBV a los cambios funcionales en las neuronas (Grubb et al., 1974), y podría por tanto servir para detectar con anterioridad los cambios funcionales en estos pacientes asintomáticos. A este respecto, según nuestros resultados, el CBF es un biomarcador más temprano que el CBV para las anomalías hemodinámicas en las fases prodrómicas de AD.

Por último, el estudio combinado de técnicas de RM (estructural, perfusión y difusión) ha permitido comprobar si la pérdida de perfusión observada en el córtex frontal y parietotemporal en los pacientes con DCL y EA tenían o no una relación directa con la atrofia en la región medial de los lóbulos temporales o con los daños en las fibras de SB que conectan estas regiones. De acuerdo a la hipótesis de la desconexión (Jobst et al., 1992; Matsuda, 2001; Mielke et al., 1996; A. D. Smith, 2002), la pérdida de flujo sanguíneo en las regiones frontales y parietotemporales podría deberse a una disminución de la actividad neuronal como consecuencia de una reducción de “inputs” neuronales desde los lóbulos temporlales mediales debido a la atrofia en esta zona. A este respecto,

se ha observado que la disminución de la perfusión sanguínea en las regiones parietales de los pacientes de DCL que progresaron a EA correlaba con cambios microestructurales en las fibras de SB que conectaban las regiones hipoperfundidas con las regiones mediales de los lóbulos temporales, pero no con la atrofia en esta región, como se había sugerido en la literatura. Estos resultados avalan la hipótesis de la desconexión, pero abren una nueva línea de investigación en terapias protectoras de la microestructura de las fibras de SB al descartar una relación directa entre hipoperfusión y atrofia cortical. En cambio, la pérdida de perfusión en las regiones parietotemporales y frontales en los pacientes de EA con demencia leve no mostró ninguna relación con los daños en las fibras de SB, lo que sugiere una etiología diferente a la desconexión para estas alteraciones en la perfusión. Estos resultados instan a continuar en la investigación de la EA desde un punto de vista de patología mixta (vascular y neuronal). Según los estudios clinicopatológicos de las últimas dos décadas las demencias de origen mixto serían las más comunes en edades avanzadas (Iadecola, 2013).

Durante el desarrollo de este trabajo nos hemos encontrado con ciertas limitaciones que merece la pena comentar. Por una parte, hay que tener en consideración que el tamaño de la muestra es reducido, especialmente en el caso del estudio con DTI, por lo que la potencia estadística de los resultados se ha podido ver comprometido; en todo caso, hay que resaltar que tamaños muestrales semejantes han sido empleados con éxito en trabajos ya publicados (Liu et al., 2011). Además no todos los pacientes completaron la adquisición de las tres modalidades de imagen, por lo que la muestra ha sido ligeramente diferente en los tres capítulos fundamentales de la tesis. Finalmente, también hay que tener en cuenta que se han estudiado dos fases de la enfermedad en dos grupos diferentes en lugar de llevar a cabo, como habría sido óptimo, un estudio de imagen longitudinal.

La principal fortaleza de nuestro estudio es la naturaleza multimodal de nuestros datos y el seguimiento clínico que se ha hecho de todos los pacientes durante varios años, lo que ha permitido reclasificar a los pacientes en los distintos grupos según su evolución clínica a lo largo del estudio.

Esta tesis doctoral abre el camino a nuevos protocolos de diagnóstico precoz mediante la utilización de técnias de imagen médica avanzadas que permitan mejorar la detección temprana de la EA y mejorar la valoración de la eficiancia de terapias en desarrollo. De igual forma, contribuye a esclarecer la existencia de un sustrato físico en la desconexión entre regiones hipoperfundidas y el lóbulo temporal medial, siendo esta hipótesis una novedosa línea de investigación sobre la que se está haciendo énfasis en publicaciones recientes en este campo.

8 CONCLUSIONES

Las conclusiones más importantes del trabajo son las siguientes:

1) Se ha encontrado una región de referencia para la normalización de intensidad de mapas paramétricos de perfusión (CBF) obtenidos con RM que facilita el hallazgo de alteraciones hemodinámicas en pacientes de EA en fase temprana. De entre las tres regiones de referencia estudiadas (cerebelo, sustancia blanca total y sustancia gris cortical total), la sustancia gris cortical total resultó ser la región de referencia óptima para la normalización de los mapas:

    - Los valores medios de CBF para la sustancia gris cortical total mostraron un menor sesgo entre grupos patológicos y controles.

    - La normalización por SG cortical total mostró la mayor reducción de variabilidad en intensidad.

    - La normalización por SG cortical total permitió la detección de un mayor número de regiones cerebrales con alteraciones hemodinámicas en los pacientes de EA.

    - El patrón de alteraciones hemodinámicas encontrado tras la normalización por sustancia gris cortical total presentó una mayor coherencia con la interpretación clínica de la patología.

2) El CBF resultó ser un biomarcador más temprano que el CBV para las anomalías hemodinámicas en las fases prodrómicas de AD.

    - Los pacientes con DCL que progresaron a demencia tipo Alzheimer mostraron diferencias significativas con respecto a los sujetos control para valores de CBF pero no de CBV.

    - Los pacientes de EA con demencia leve mostraron diferencias significativas para los valores de CBF pero también para CBV.

- Ni los valores de CBF ni los de CBV mostraron correlación alguna con la atrofia en aquellas regiones cerebrales donde la atrofia y las alteraciones hemodinámicas coexistieron.

- En los pacientes de DCL se observó una alta correlación entre el aumento de CBF y la pérdida de grosor cortical en la girificación parahipocampal derecha.

3) La disminución de perfusión sanguínea en las regiones parietales de los pacientes de DCL que progresaron a EA parece estar relacionada con el daño en las fibras de SB que conectan dichas regiones con el lóbulo temporal medial, apoyando así la hipótesis de la desconexión. En cambio, la pérdida de perfusión en las regiones parietotemporales y frontales en los pacientes de EA no mostró ninguna relación con los daños en estas fibras, lo que sugiere una etiología diferente para estas alteraciones.

   - Tanto los pacientes con DCL que progresaron a Alzheimer como los pacientes de EA mostraron cambios microestructurales en las fibras de SB de algunos tractos del sistema límbico y en algunas regiones del cuerpo calloso, sugiriendo una alteración física de las conexiones cortico-corticales intra e inter lóbulo.

   - No se encontró una correlación entre la pérdida de CBF en las cortezas parietotemporales y frontales y la disminución del grosor cortical en las regiones atrofiadas de los lóbulos temporales mediales en ninguno de los grupos patológicos.

   - En el grupo de pacientes con DCL que progresaron a Alzheimer, los déficits de perfusión sanguínea en la corteza parietal presentaron una fuerte asociación con los cambios microestructurales de las fibras de SB que conectan las regiones hipoperfundidas con las regiones atrofiadas de los lóbulos temporales mediales.

- La ausencia de correlación entre el grosor cortical en las regiones atrofiadas de los lóbulos temporales y la pérdida de FA en los tractos de SB del sistema límbico sugiere que los cambios microestructurales en estos tractos no están directamente asociados a la atrofia producida en los lóbulos temporales mediales.

PUBLICACIONES

Como primera autora

Revistas internacionales

M Lacalle-Aurioles, JM Mateos-Pérez, J Guzmán de Villoria, J Olazarán, I Cruz, Y Alemán-Gómez, E Martino, M Desco. Cerebral blood flow is an earlier indicator of perfusion abnormalities than cerebral blood volume in Alzheimer's disease. ***J Cereb Blood Flow Metab***. 2014 Jan 15. doi: 10.1038/jcbfm.2013.241.

M Lacalle-Aurioles, Y Alemán-Gómez, J Guzmán de Villoria, J Olazarán, I Cruz, JM Mateos-Pérez, E Martino, M Desco. (2013). Is the cerebellum the optimal reference region for intensity normalization of perfusion MR studies in early Alzheimer's disease. ***PLoS One***. 2013 Dec 27;8(12):e81548. doi: 10.1371/journal.pone.0081548.

M Lacalle-Aurioles, FJ Navas-Sánchez, Y Alemán-Gómez, J Olazarán, J Guzmán de Villoria, JM Mateos-Pérez, I Cruz, M Desco. The disconnection hypothesis in Alzheimer's disease studied through multimodal MRI: structural, perfusion and diffusion tensor imaging. (submitted to ***Brain***)

M Lacalle-Aurioles, Y Alemán-Gómez, J Guzmán de Villoria, I Cruz, J Olazarán, M Desco. Cortical volume, surface area or mean thickness; seeking a descriptor of cortical deficits in Alzheimer's disease. (in preparation for ***AJNR***)

Proceedings

M. Lacalle-Aurioles, Y. Alemán-Gómez, J. Guzmán-De-Villoria, J. Olazarán, I. Cruz, J.M. Mateos-Pérez, E. Martino, and M. Desco. The importance of a valid reference region for intensity normalization of perfusion MR studies in early Alzheimer's disease. Poster presentation delivered at XIII Mediterranean Conference on Medical and Biological Engineering and Computing - MEDICON 2013. pp.218-221. I.S.B.N. 978-3-319-00846-2.

M. La Calle, S. Reig, J. Guzmán de Villoria, J. M. Mateos-Pérez, J. Olazarán, I. Cruz, E. Martino, J. Navas, V. Rebollo, L. Sánchez, M. Desco. Normalización de datos de perfusión por RM: resultados contradictorios en las diferencias entre pacientes de Alzheimer y controles dependiendo de la región de referencia. Actas del XXVII Congreso Anual de la Sociedad Española de Ingeniería Biomédica 2009. pp.349-52 I.S.B.N. 978-84-608-0990-6.

Ponencias en congresos

M. Lacalle-Aurioles, Y. Alemán-Gómez, J. Guzmán-De-Villoria, J. Olazarán, I. Cruz, J.M. Mateos-Pérez, E. Martino, and M. Desco. The importance of a valid reference region for intensity normalization of perfusion MR studies in early Alzheimer's disease. Poster presentation delivered at XIII Mediterranean Conference on Medical and Biological Engineering and Computing – MEDICON, Sevilla, Spain, September 2013.

M LaCalle; J A Guzmán-De-Villoria; S Reig; J Mateos-Pérez; J Olazarán; M Desco-Menéndez. Controversy in differences of brain perfusion data between Alzheimer's disease patients and healthy controls could be due to the choice of reverence region for normalization. Radiological Society of North America Abtracts. E-Poster presentation delivered at RSNA 97th Scientific Assembly and Annual Meeting. Chicago, California, USA, December 2011.

M LaCalle; J A Guzman-de-Villoria; Y Alemán; I Cruz; E Martino; M Desco-Menendez. Volume, Surface, or Thickness: What Is the Best Descriptor of Cortical Deficits in Alzheimers Disease? Radiological Society of North America Abtracts. E-Poster presentation delivered at RSNA 97th Scientific Assembly and Annual Meeting. Chicago, California, USA, December 2011.

M. LaCalle, S. Reig, J. Guzmán de Villoria, J. Olazarán, I. Cruz, E. Martino, J. M. Mateos-Pérez, J. Navas, M. Desco. Comparison of cortical volume and perfusion MRI data in Alzheimer's patients and controls. Poster presentation delivered at OHBM 16th Annual Meeting. Barcelona, Spain. June 2010.

M. La Calle, S. Reig, J. Guzmán de Villoria, J. M. Mateos-Pérez, J. Olazarán, I. Cruz, E. Martino, J. Navas, V. Rebollo, L. Sánchez, M. Desco. Normalización de datos de perfusión por RM: resultados contradictorios en las diferencias entre pacientes de Alzheimer y controles dependiendo de la región de referencia. Poster presentation delivered at XXVII Congreso Anual de la Sociedad Española de Ingeniería Biomédica - CASEIB Cadiz, Spain. November 2009.

Como coautora

Revistas internacionales

Martino ME, de Villoria JG, **Lacalle-Aurioles M**, Olazarán J, Cruz I, Navarro E, García-Vázquez V, Carreras JL, Desco M**.** (2013)**.** Comparison of different methods of spatial normalization of FDG-PET brain images in the voxel-wise analysis of MCI patients and controls. ***Annals of Nuclear Medicine*** Aug;27(7):600-9. doi: 10.1007/s12149-013-0723-7.

Proceedings

M. E. Martino, V. García-Vázquez, **M. Lacalle-Aurioles**, J. Olazarán, J. Guzmán de Villoria, I. Cruz, J. L. Carreras, M. Desco. Spatial normalization in voxel-wise analysis of FDG-PET brain images. Oral presentation delivered at XIII Mediterranean Conference on Medical and Biological Engineering and Computing - MEDICON 2013. pp. 447-451 I.S.B.N. 978-3-319-00846-2.

E Martino, S Reig, J Guzmán de Villoria, J Olazarán, I Cruz, **M LaCalle**, V García, M Desco Diferentes métodos de normalización espacial en el análisis SPM de imágenes PET - FDG entre un grupo de sujetos control y un grupo de pacientes con DCL. CASEIB 2010 I.S.B.N. 978-84-8058-1

J. Navas, S. Reig, J. Janssen, Y. Alemán, **M. La Calle**, E. Martino, V. Rebollo, L. Sánchez, M. Desco. Repetibilidad intra- e inter-observador en la cuantificación de valores de FA del cuerpo calloso utilizando métodos de tractografía en imágenes de DTI Actas del XXVII Congreso Anual de la Sociedad Española de Ingeniería Biomédica 2009 pp.177-80 I.S.B.N. 978-84-608-0990-6.

Ponencias en congresos

M. E. Martino, V. García-Vázquez, **M. Lacalle-Aurioles**, J. Olazarán, J. Guzmán de Villoria, I. Cruz, J. L. Carreras, M. Desco. Spatial normalization in voxel-wise analysis of FDG-PET brain images. Oral presentation delivered at XIII Mediterranean Conference on Medical and Biological Engineering and Computing - MEDICON, Sevilla, Spain, September 2013.

E Martino, S Reig, J Guzmán de Villoria, J Olazarán, I Cruz, **M LaCalle**, V García1, M Desco Diferentes métodos de normalización espacial en el análisis SPM de imágenes PET - FDG entre un grupo de sujetos control y un grupo de pacientes con DCL. Oral presentation delivered at XXVIII Congreso Anual de la Sociedad Española de Ingeniería Biomédica - CASEIB 2010. Madrid, Spain. November 2010.

E Martino, Y Alemán, S Reig, J Guzmán de Villoria, J Olazarán, **M LaCalle**, I Cruz, V García, M Desco. Effect of spatial normalization in the SPM analysis of PET images of MCI patients and controls. Poster presentation delivered at OHBM 16th Annual Meeting. Barcelona, Spain. June 2010.

J. Navas, S. Reig, J. Janssen, Y. Alemán, **M. La Calle**, E. Martino, V. Rebollo, L. Sánchez, M. Desco. Repetibilidad intra- e inter-observador en la cuantificación de valores de FA del cuerpo calloso utilizando métodos de tractografía en imágenes de DTI. Oral presentation delivered at XXVII Congreso Anual de la Sociedad Española de Ingeniería Biomédica - CASEIB Cadiz, Spain. November 2009.

S. Reig, J. Guzmán de Villoria, J. Olazarán, **M. Lacalle**, E. Martino, J.M. Mateos, I. Cruz, V. García, and M. Desco. Choice of reference region for the normalization of brain Cerebral Blood Volume maps in comparative studies. NeuroImage, Volume 47, Supplement 1, July 2009, p. S125. Poster presentation delivered at OHBM 15th Annual Meeting. San Francisco, California. USA. June 2009.

S. Reig, J.A. Guzmán de Villoria, J. Olazarán, I. Cruz, **M. Lacalle**, E. Navarro, D. Ezpeleta, J.M. Mateos, V. García-Vázquez, E. Martino, and M. Desco. Use of the Talairach Proportional Grid System for ROI Quantification of Cerebral Blood Volume Maps of the Brain. Proc Intl Soc Mag Reson Med, 2009, p.3350. E-poster presentation delivered at ISMRM 17th Scientific Meeting & Exhibition. Honolulu, Hawai, USA. April 2009.

Olazarán Rodríguez, J. Reig Redondo, S. Guzmán de Villoria, J. Cruz Orduña, I. Mateos Pérez, J.M. **Lacalle Aurioles, M**. Navarro Merino, E. Desco Menéndez, M. Resonancia magnética de perfusión en la enfermedad de Alzheimer inicial. Poster presentation delivered at LX Reunión Anual de la Sociedad Española de Neurología. Barcelona, Spain. November 2008.

REFERENCIAS

Alsop DC, Casement M, de Bazelaire C, Fong T, Press DZ. Hippocampal hyperperfusion in Alzheimer's disease. Neuroimage 2008; 42: 1267–1274.

Alsop DC, Detre JA, Grossman M. Assessment of cerebral blood flow in Alzheimer's disease by spin-labeled magnetic resonance imaging. Ann Neurol 2000; 47: 93–100.

Alzheimer A. Über eine eigenartige Erkrankung der Hirnrinde. Allg. Zeitschrift für Psychiatr. 1907; 64: 146–148.

American Psychiatric Association. Diagnostic and Statistical Manual of Mental Disorders. Fourth Edi. Washington, DC: American Psychiatric Publishing, Inc.; 2000.

Ballard C, Sorensen S, Sharp S. Pharmacological therapy for people with Alzheimer's disease: the balance of clinical effectiveness, ethical issues and social and healthcare costs. J. Alzheimers. Dis. 2007; 12: 53–9.

Bammer R, Skare S, Newbould R, Liu C, Thijs V, Ropele S, et al. Foundations of advanced magnetic resonance imaging. NeuroRx 2005; 2: 167–196.

Barkhof F, Polvikoski TM, van Straaten EC, Kalaria RN, Sulkava R, Aronen HJ, et al. The significance of medial temporal lobe atrophy: a postmortem MRI study in the very old. Neurology 2007; 69: 1521–1527.

Basser PJ, Mattiello J, LeBihan D. Estimation of the effective self-diffusion tensor from the NMR spin echo. J Magn Reson B 1994; 103: 247–254.

Basser PJ, Pierpaoli C. Microstructural and physiological features of tissues elucidated by quantitative-diffusion-tensor MRI. J Magn Reson B 1996; 111: 209–219.

Bech-Azeddine R, Hogh P, Juhler M, Gjerris F, Waldemar G. Idiopathic normal-pressure hydrocephalus: clinical comorbidity correlated with cerebral biopsy findings and outcome of cerebrospinal fluid shunting. J Neurol Neurosurg Psychiatry 2007; 78: 157–161.

Van Beek AHEA, Claassen JAHR. The cerebrovascular role of the cholinergic neural system in Alzheimer's disease. Behav. Brain Res. 2011; 221: 537–542.

Behrens TE, Woolrich MW, Jenkinson M, Johansen-Berg H, Nunes RG, Clare S, et al. Characterization and propagation of uncertainty in diffusion-weighted MR imaging. Magn Reson Med 2003; 50: 1077–1088.

Bell MA, Ball MJ. Morphometric comparison of hippocampal microvasculature in ageing and demented people: diameters and densities. Acta Neuropathol. 1981; 53: 299–318.

Bennett DA, Schneider JA, Arvanitakis Z, Kelly JF, Aggarwal NT, Shah RC, et al. Neuropathology of older persons without cognitive impairment from two community-based studies. Neurology 2006; 66: 1837–1844.

Bobinski M, de Leon MJ, Wegiel J, Desanti S, Convit A, Saint Louis LA, et al. The histological validation of post mortem magnetic resonance imaging-determined hippocampal volume in Alzheimer's disease. Neuroscience 2000; 95: 721–725.

Bocti C, Rockel C, Roy P, Gao F, Black SE. Topographical patterns of lobar atrophy in frontotemporal dementia and Alzheimer's disease. Dement Geriatr Cogn Disord 2006; 21: 364–372.

Borghammer P, Jonsdottir KY, Cumming P, Ostergaard K, Vang K, Ashkanian M, et al. Normalization in PET group comparison studies--the importance of a valid reference region. Neuroimage 2008; 40: 529–540.

Bozzao A, Floris R, Baviera ME, Apruzzese A, Simonetti G. Diffusion and perfusion MR imaging in cases of Alzheimer's disease: correlations with cortical atrophy and lesion load. AJNR Am J Neuroradiol 2001; 22: 1030–1036.

Braak H, Braak E. Neuropathological stageing of Alzheimer-related changes. Acta Neuropathol 1991; 82: 239–259.

Caroli A, Testa C, Geroldi C, Nobili F, Barnden LR, Guerra UP, et al. Cerebral perfusion correlates of conversion to Alzheimer's disease in amnestic mild cognitive impairment. J Neurol 2007; 254: 1698–1707.

Carr DB, Goate A, Phil D, Morris JC. Current concepts in the pathogenesis of Alzheimer's disease. Am J Med 1997; 103: 3S–10S.

Chan D, Janssen JC, Whitwell JL, Watt HC, Jenkins R, Frost C, et al. Change in rates of cerebral atrophy over time in early-onset Alzheimer's disease: longitudinal MRI study. Lancet 2003; 362: 1121–2.

Chui HC, Zarow C, Mack WJ, Ellis WG, Zheng L, Jagust WJ, et al. Cognitive impact of subcortical vascular and Alzheimer's disease pathology. Ann Neurol 2006; 60: 677–687.

Clement F, Belleville S. Compensation and disease severity on the memory-related activations in mild cognitive impairment. Biol Psychiatry 2010; 68: 894–902.

Collignon A, Maes F, Delaere D, Vandermeulen D, Suetens P, Marchal G. Automated multi-modality image registration based on information theory. In: Information Processing in Medical Imaging. Amsterdam: Kluwer Academic Publishers; 1995.

Cooper RL, Chang DB, Young AC, Martin CJ, Ancker-Johnson D. Restricted diffusion in biophysical systems. Experiment. Biophys. J. 1974; 14: 161–77.

Cummings JL, Cole G. Alzheimer disease. JAMA 2002; 287: 2335–8.

Cummings JL. Integrating symptomatic- and disease-modifying treatments. CNS Spectr 2008; 13: 28–30.

Dai W, Lopez OL, Carmichael OT, Becker JT, Kuller LH, Gach HM. Mild cognitive impairment and alzheimer disease: patterns of altered cerebral blood flow at MR imaging. Radiology 2009; 250: 856–866.

Dale AM, Fischl B, Sereno MI. Cortical surface-based analysis. I. Segmentation and surface reconstruction. Neuroimage 1999; 9: 179–194.

Davis DG, Schmitt FA, Wekstein DR, Markesbery WR. Alzheimer neuropathologic alterations in aged cognitively normal subjects. J Neuropathol Exp Neurol 1999; 58: 376–388.

DeKosky ST, Marek K. Looking backward to move forward: early detection of neurodegenerative disorders. Science (80-.). 2003; 302: 830–834.

Delacourte A. Biochemical and molecular characterization of neurofibrillary degeneration in frontotemporal dementias. Dement Geriatr Cogn Disord 1999; 10 Suppl 1: 75–79.

Desikan RS, Segonne F, Fischl B, Quinn BT, Dickerson BC, Blacker D, et al. An automated labeling system for subdividing the human cerebral cortex on MRI scans into gyral based regions of interest. Neuroimage 2006; 31: 968–980.

Diamant M, Harms MP, Immink R V, Van Lieshout JJ, Van Montfrans GA. Twenty-four-hour non-invasive monitoring of systemic haemodynamics and cerebral blood flow velocity in healthy humans. Acta Physiol Scand 2002; 175: 1–9.

Dickerson BC, Sperling RA. Functional abnormalities of the medial temporal lobe memory system in mild cognitive impairment and Alzheimer's disease: insights from functional MRI studies. Neuropsychologia 2008; 46: 1624–1635.

Dubois B, Feldman HH, Jacova C, Cummings JL, Dekosky ST, Barberger-Gateau P, et al. Revising the definition of Alzheimer's disease: a new lexicon. Lancet Neurol 2010; 9: 1118–1127.

Duron E, Hanon O. Vascular risk factors, cognitive decline, and dementia. Vasc. Health Risk Manag. 2008; 4: 363–81.

Essig M, Nguyen TB, Shiroishi MS, Saake M, Provenzale JM, Enterline DS, et al. Perfusion MRI: The Five Most Frequently Asked Clinical Questions. AJR Am J Roentgenol 2013; 201: W495–510.

Fellgiebel A, Schermuly I, Gerhard A, Keller I, Albrecht J, Weibrich C, et al. Functional relevant loss of long association fibre tracts integrity in early Alzheimer's disease. Neuropsychologia 2008; 46: 1698–1706.

Fiedler U, Augustin HG. Angiopoietins: a link between angiogenesis and inflammation. Trends Immunol 2006; 27: 552–558.

Fischl B, Dale AM. Measuring the thickness of the human cerebral cortex from magnetic resonance images. Proc Natl Acad Sci U S A 2000; 97: 11050–11055.

Fischl B, Salat DH, Busa E, Albert M, Dieterich M, Haselgrove C, et al. Whole brain segmentation: automated labeling of neuroanatomical structures in the human brain. Neuron 2002; 33: 341–355.

Folstein MF, Folstein SE, McHugh PR. "Mini-mental state". A practical method for grading the cognitive state of patients for the clinician. J Psychiatr Res 1975; 12: 189–198.

Gibby WA. Basic principles of magnetic resonance imaging. Neurosurg Clin N Am 2005; 16: 1–64.

González RG, Fischman AJ, Guimaraes AR, Carr CA, Stern CE, Halpern EF, et al. Functional MR in the evaluation of dementia: correlation of abnormal dynamic cerebral blood volume measurements with changes in cerebral metabolism on positron emission tomography with fludeoxyglucose F 18. AJNR. Am. J. Neuroradiol. 1995; 16: 1763–1770.

Gordon JH, Robert FL, Andrew S, Camper DE, Tammy MS, Deborah A, et al. Dynamic susceptibility Contrast MS Imaging of Regional Cerebral Blood Volume in Alzheimer Disease: A promisig Alternative to Nuclear Medicine. Am. J. Neuroradiol. 1998; 19: 1727–1732.

Grubb RL, Raichle ME, Eichling JO, Ter-Pogossian MM. The Effects of Changes in PaCO2 Cerebral Blood Volume, Blood Flow, and Vascular Mean Transit Time. Stroke 1974; 5: 630–639.

Hanyu H, Sato T, Hirao K, Kanetaka H, Iwamoto T, Koizumi K. The progression of cognitive deterioration and regional cerebral blood flow patterns in Alzheimer's disease: a longitudinal SPECT study. J Neurol Sci 2010; 290: 96–101.

Harder DR, Zhang C, Gebremedhin D. Astrocytes function in matching blood flow to metabolic activity. News Physiol Sci 2002; 17: 27–31.

Harris GJ, Lewis RF, Satlin A, English CD, Scott TM, Yurgelun-Todd DA, et al. Dynamic susceptibility contrast MR imaging of regional cerebral blood volume in Alzheimer disease: a promising alternative to nuclear medicine. AJNR Am J Neuroradiol 1998; 19: 1727–1732.

Hauser T, Schönknecht P, Thomann P a, Gerigk L, Schröder J, Henze R, et al. Regional cerebral perfusion alterations in patients with mild cognitive impairment and Alzheimer disease using dynamic susceptibility contrast MRI. Acad. Radiol. 2013; 20: 705–11.

Henry-Feugeas MC. Alzheimer's disease in late-life dementia: a minor toxic consequence of devastating cerebrovascular dysfunction. Med Hypotheses 2008; 70: 866–875.

Henry-Feugeas MC. Assessing cerebrovascular contribution to late dementia of the Alzheimer's type: the role of combined hemodynamic and structural MR analysis. J Neurol Sci 2009; 283: 44–48.

Hirao K, Ohnishi T, Hirata Y, Yamashita F, Mori T, Moriguchi Y, et al. The prediction of rapid conversion to Alzheimer's disease in mild cognitive impairment using regional cerebral blood flow SPECT. Neuroimage 2005; 28: 1014–1021.

Hirao K, Ohnishi T, Matsuda H, Nemoto K, Hirata Y, Yamashita F, et al. Functional interactions between entorhinal cortex and posterior cingulate cortex at the very early

stage of Alzheimer's disease using brain perfusion single-photon emission computed tomography. Nucl Med Commun 2006; 27: 151–156.

Huang Y-C, Liu H-L, Lee J-D, Yang J-T, Weng H-H, Lee M, et al. Comparison of arterial spin labeling and dynamic susceptibility contrast perfusion MRI in patients with acute stroke. PLoS One 2013; 8: e69085.

Hughes CP, Berg L, Danziger WL, Coben LA, Martin RL. A new clinical scale for the staging of dementia. Br J Psychiatry 1982; 140: 566–572.

Hurd MD, Martorell P, Delavande A, Mullen KJ, Langa KM. Monetary costs of dementia in the United States. N. Engl. J. Med. 2013; 368: 1326–34.

Iadecola C. The pathobiology of vascular dementia. Neuron 2013; 80: 844–66.

Ishii H, Meguro K, Yamaguchi S, Hirayama K, Tabuchi M, Mori E, et al. Different MRI findings for normal elderly and very mild Alzheimer's disease in a community: implications for clinical practice the Tajiri Project. Arch Gerontol Geriatr 2006; 42: 59–71.

Ishii K, Sasaki M, Kitagaki H, Yamaji S, Sakamoto S, Matsuda K, et al. Reduction of cerebellar glucose metabolism in advanced Alzheimer's disease. J. Nucl. … 1997; 38: 925–928.

Ito R, Mori S, Melhem ER. Diffusion tensor brain imaging and tractography. Neuroimaging Clin. N. Am. 2002; 12: 1–19.

Jackson JR, Seed MP, Kircher CH, Willoughby DA, Winkler JD. The codependence of angiogenesis and chronic inflammation. FASEB J. 1997; 11: 457–65.

Jagust W, Thisted R, Devous Sr. MD, Van Heertum R, Mayberg H, Jobst K, et al. SPECT perfusion imaging in the diagnosis of Alzheimer's disease: a clinical-pathologic study. Neurology 2001; 56: 950–956.

Jagust WJ, Zheng L, Harvey DJ, Mack WJ, Vinters H V, Weiner MW, et al. Neuropathological basis of magnetic resonance images in aging and dementia. Ann Neurol 2008; 63: 72–80.

Jakovcevic D, Harder DR. Role of astrocytes in matching blood flow to neuronal activity. Curr Top Dev Biol 2007; 79: 75–97.

Jobst KA, Smith AD, Barker CS, Wear A, King EM, Smith A, et al. Association of atrophy of the medial temporal lobe with reduced blood flow in the posterior parietotemporal cortex in patients with a clinical and pathological diagnosis of Alzheimer's disease. J Neurol Neurosurg Psychiatry 1992; 55: 190–194.

Johnson NA, Jahng GH, Weiner MW, Miller BL, Chui HC, Jagust WJ, et al. Pattern of cerebral hypoperfusion in Alzheimer disease and mild cognitive impairment measured with arterial spin-labeling MR imaging: initial experience. Radiology 2005; 234: 851–859.

Karbe H, Kertesz A, Davis J, Kemp BJ, Prato FS, Nicholson RL. Quantification of functional deficit in Alzheimer's disease using a computer-assisted mapping program for 99mTc-HMPAO SPECT. Neuroradiology 1994; 36: 1–6.

Kitaguchi H, Ihara M, Saiki H, Takahashi R, Tomimoto H. Capillary beds are decreased in Alzheimer's disease, but not in Binswanger's disease. Neurosci. Lett. 2007; 417: 128–131.

Knopman DS, DeKosky ST, Cummings JL, Chui H, Corey-Bloom J, Relkin N, et al. Practice parameter: diagnosis of dementia (an evidence-based review). Report of the Quality Standards Subcommittee of the American Academy of Neurology. Neurology 2001; 56: 1143–53.

Knopman DS, Parisi JE, Salviati A, Floriach-Robert M, Boeve BF, Ivnik RJ, et al. Neuropathology of cognitively normal elderly. J Neuropathol Exp Neurol 2003; 62: 1087–1095.

Koehler RC, Roman RJ, Harder DR. Astrocytes and the regulation of cerebral blood flow. Trends Neurosci 2009; 32: 160–169.

Kolbitsch C, Lorenz IH, Hormann C, Schocke M, Kremser C, Zschiegner F, et al. A subanesthetic concentration of sevoflurane increases regional cerebral blood flow and regional cerebral blood volume and decreases regional mean transit time and regional cerebrovascular resistance in volunteers. Anesth Analg 2000; 91: 156–162.

Kuperberg GR, Broome MR, McGuire PK, David AS, Eddy M, Ozawa F, et al. Regionally localized thinning of the cerebral cortex in schizophrenia. Arch Gen Psychiatry 2003; 60: 878–888.

De la Torre JC. Alzheimer disease as a vascular disorder: nosological evidence. Stroke 2002; 33: 1152–1162.

De la Torre JC. Is Alzheimer's disease a neurodegenerative or a vascular disorder? Data, dogma, and dialectics. Lancet Neurol 2004; 3: 184–190.

Lecrux C, Hamel E. The neurovascular unit in brain function and disease. Acta Physiol 2011; 203: 47–59.

De Leon MJ, George AE, Golomb J, Tarshish C, Convit A, Kluger A, et al. Frequency of hippocampal formation atrophy in normal aging and Alzheimer's disease. Neurobiol Aging 1997; 18: 1–11.

Li X, Tian J, Li E, Wang X, Dai J, Ai L. Adaptive total linear least square method for quantification of mean transit time in brain perfusion MRI. Magn Reson Imaging 2003; 21: 503–510.

Liu Y, Spulber G, Lehtimaki KK, Kononen M, Hallikainen I, Grohn H, et al. Diffusion tensor imaging and tract-based spatial statistics in Alzheimer's disease and mild cognitive impairment. Neurobiol Aging 2011; 32: 1558–1571.

Lyseng-Williamson KA, Plosker GL. Galantamine: a pharmacoeconomic review of its use in Alzheimer's disease. Pharmacoeconomics 2002; 20: 919–42.

Maccioni RB, Munoz JP, Barbeito L. The molecular bases of Alzheimer's disease and other neurodegenerative disorders. Arch Med Res 2001; 32: 367–381.

Matsuda H. Cerebral blood flow and metabolic abnormalities in Alzheimer's disease. Ann. Nucl. Med. 2001; 15: 85–92.

Matsuda H. Role of neuroimaging in Alzheimer's disease, with emphasis on brain perfusion SPECT. J Nucl Med 2007; 48: 1289–1300.

McDonald CR, Gharapetian L, McEvoy LK, Fennema-Notestine C, Hagler Jr. DJ, Holland D, et al. Relationship between regional atrophy rates and cognitive decline in mild cognitive impairment. Neurobiol Aging 2012; 33: 242–253.

McKhann G, Drachman D, Folstein M, Katzman R, Price D, Stadlan EM. Clinical diagnosis of Alzheimer's disease: report of the NINCDS-ADRDA Work Group under the auspices of Department of Health and Human Services Task Force on Alzheimer's Disease. Neurology 1984; 34: 939–944.

Mielke MM, Kozauer N a, Chan KCG, George M, Toroney J, Zerrate M, et al. Regionally-specific diffusion tensor imaging in mild cognitive impairment and Alzheimer's disease. Neuroimage 2009; 46: 47–55.

Mielke R, Schröder R, Fink GR, Kessler J, Herholz K, Heiss WD. Regional cerebral glucose metabolism and postmortem pathology in Alzheimer's disease. Acta Neuropathol. 1996; 91: 174–9.

Mori S, Oishi K, Jiang H, Jiang L, Li X, Akhter K, et al. Stereotaxic white matter atlas based on diffusion tensor imaging in an ICBM template. Neuroimage 2008; 40: 570–82.

Mueller SG, Schuff N, Weiner MW. Evaluation of treatment effects in Alzheimer's and other neurodegenerative diseases by MRI and MRS. NMR Biomed 2006; 19: 655–668.

Nagata K, Kondoh Y, Atchison R, Sato M, Satoh Y, Watahiki Y, et al. Vascular and metabolic reserve in Alzheimer's disease. Neurobiol Aging 2000; 21: 301–307.

Nakano S, Asada T, Matsuda H, Uno M, Takasaki M. Donepezil hydrochloride preserves regional cerebral blood flow in patients with Alzheimer's disease. J Nucl Med 2001; 42: 1441–1445.

Nelson PT, Braak H, Markesbery WR. Neuropathology and cognitive impairment in Alzheimer disease: a complex but coherent relationship. J. Neuropathol. Exp. Neurol. 2009; 68: 1–14.

Paulson OB, Hasselbalch SG, Rostrup E, Knudsen GM, Pelligrino D. Cerebral blood flow response to functional activation. J. Cereb. Blood Flow Metab. 2010; 30: 2–14.

Petersen RC, Smith GE, Waring SC, Ivnik RJ, Tangalos EG, Kokmen E. Mild cognitive impairment: clinical characterization and outcome. Arch Neurol 1999; 56: 303–308.

Petrella JR, Coleman RE, Doraiswamy PM. Neuroimaging and early diagnosis of Alzheimer disease: a look to the future. Radiology 2003; 226: 315–336.

Petzold GC, Murthy VN. Role of astrocytes in neurovascular coupling. Neuron 2011; 71: 782–97.

Price JL, Morris JC. Tangles and plaques in nondemented aging and "preclinical" Alzheimer's disease. Ann Neurol 1999; 45: 358–368.

Prince M, Bryce R, Albanese E, Wimo A, Ribeiro W, Ferri CP. The global prevalence of dementia: a systematic review and metaanalysis. Alzheimers. Dement. 2013; 9: 63–75.e2.

Reitz C, Brayne C, Mayeux R. Epidemiology of Alzheimer disease. Nat Rev Neurol 2011; 7: 137–152.

Rempp KA, Brix G, Wenz F, Becker CR, Guckel F, Lorenz WJ. Quantification of regional cerebral blood flow and volume with dynamic susceptibility contrast-enhanced MR imaging. Radiology 1994; 193: 637–641.

Rentz DM, Locascio JJ, Becker JA, Moran EK, Eng E, Buckner RL, et al. Cognition, reserve, and amyloid deposition in normal aging. Ann Neurol 2010; 67: 353–364.

Rosas HD, Liu AK, Hersch S, Glessner M, Ferrante RJ, Salat DH, et al. Regional and progressive thinning of the cortical ribbon in Huntington's disease. Neurology 2002; 58: 695–701.

Rose SE, Chen F, Chalk JB, Zelaya FO, Strugnell WE, Benson M, et al. Loss of connectivity in Alzheimer's disease: an evaluation of white matter tract integrity with colour coded MR diffusion tensor imaging. J Neurol Neurosurg Psychiatry 2000; 69: 528–530.

Rose SE, McMahon KL, Janke AL, O'Dowd B, de Zubicaray G, Strudwick MW, et al. Diffusion indices on magnetic resonance imaging and neuropsychological performance in amnestic mild cognitive impairment. J Neurol Neurosurg Psychiatry 2006; 77: 1122–1128.

Salminen A, Ojala J, Kauppinen A, Kaarniranta K, Suuronen T. Inflammation in Alzheimer's disease: amyloid-beta oligomers trigger innate immunity defence via pattern recognition receptors. Prog Neurobiol 2009; 87: 181–194.

Smith AD. Imaging the progression of Alzheimer pathology through the brain. Proc Natl Acad Sci U S A 2002; 99: 4135–4137.

Smith EE, Greenberg SM. Beta-amyloid, blood vessels, and brain function. Stroke 2009; 40: 2601–2606.

Smith SM, Jenkinson M, Woolrich MW, Beckmann CF, Behrens TE, Johansen-Berg H, et al. Advances in functional and structural MR image analysis and implementation as FSL. Neuroimage 2004; 23 Suppl 1: S208–19.

Smith SM. Fast robust automated brain extraction. Hum Brain Mapp 2002; 17: 143–155.

Soonawala D, Amin T, Ebmeier KP, Steele JD, Dougall NJ, Best J, et al. Statistical parametric mapping of (99m)Tc-HMPAO-SPECT images for the diagnosis of Alzheimer's disease: normalizing to cerebellar tracer uptake. Neuroimage 2002; 17: 1193–1202.

Stefani A, Sancesario G, Pierantozzi M, Leone G, Galati S, Hainsworth AH, et al. CSF biomarkers, impairment of cerebral hemodynamics and degree of cognitive decline in Alzheimer's and mixed dementia. J Neurol Sci 2009; 283: 109–115.

Stenset V, Johnsen L, Kocot D, Negaard A, Skinningsrud A, Gulbrandsen P, et al. Associations between white matter lesions, cerebrovascular risk factors, and low CSF Abeta42. Neurology 2006; 67: 830–833.

Talbot PR, Lloyd JJ, Snowden JS, Neary D, Testa HJ. Choice of reference region in the quantification of single-photon emission tomography in primary degenerative dementia. Eur J Nucl Med 1994; 21: 503–508.

Talbot PR, Lloyd JJ, Snowden JS, Neary D, Testa HJ. A clinical role for 99mTc-HMPAO SPECT in the investigation of dementia? J Neurol Neurosurg Psychiatry 1998; 64: 306–313.

Teipel SJ, Stahl R, Dietrich O, Schoenberg SO, Perneczky R, Bokde AL, et al. Multivariate network analysis of fiber tract integrity in Alzheimer's disease. Neuroimage 2007; 34: 985–995.

Tian J, Shi J, Smallman R, Iwatsubo T, Mann DM. Relationships in Alzheimer's disease between the extent of Abeta deposition in cerebral blood vessel walls, as cerebral amyloid angiopathy, and the amount of cerebrovascular smooth muscle cells and collagen. Neuropathol Appl Neurobiol 2006; 32: 332–340.

Tomlinson BE, Blessed G, Roth M. Observations on the brains of non-demented old people. J Neurol Sci 1968; 7: 331–356.

Uh J, Lewis-Amezcua K, Martin-Cook K, Cheng Y, Weiner M, Diaz-Arrastia R, et al. Cerebral blood volume in Alzheimer's disease and correlation with tissue structural integrity. Neurobiol Aging 2009; 31: 2038–2046.

Vemuri P, Gunter JL, Senjem ML, Whitwell JL, Kantarci K, Knopman DS, et al. Alzheimer's disease diagnosis in individual subjects using structural MR images: validation studies. Neuroimage 2008; 39: 1186–1197.

Villemagne VL, Pike KE, Chetelat G, Ellis KA, Mulligan RS, Bourgeat P, et al. Longitudinal assessment of Abeta and cognition in aging and Alzheimer disease. Ann Neurol 2011; 69: 181–192.

Wakana S, Jiang H, Nagae-Poetscher LM, van Zijl PC, Mori S. Fiber tract-based atlas of human white matter anatomy. Radiology 2004; 230: 77–87.

Wilkinson BL, Cramer PE, Varvel NH, Reed-Geaghan E, Jiang Q, Szabo A, et al. Ibuprofen attenuates oxidative damage through NOX2 inhibition in Alzheimer's disease. Neurobiol Aging 2012; 33: 197.e21–e32.

Winblad B, Palmer K, Kivipelto M, Jelic V, Fratiglioni L, Wahlund LO, et al. Mild cognitive impairment--beyond controversies, towards a consensus: report of the International Working Group on Mild Cognitive Impairment. J Intern Med 2004; 256: 240–246.

Yoshiura T, Hiwatashi A, Yamashita K, Ohyagi Y, Monji A, Takayama Y, et al. Simultaneous measurement of arterial transit time, arterial blood volume, and cerebral blood flow using arterial spin-labeling in patients with Alzheimer disease. AJNR Am J Neuroradiol 2009; 30: 1388–1393.

Zhang B, Xu Y, Zhu B, Kantarci K. The role of diffusion tensor imaging in detecting microstructural changes in prodromal Alzheimer's disease. CNS Neurosci. Ther. 2014; 20: 3–9.

Zhang Y, Schuff N, Jahng G-H, Bayne W, Mori S, Schad L, et al. Diffusion tensor imaging of cingulum fibers in mild cognitive impairment and Alzheimer disease. Neurology 2007; 68: 13–9.

Zimny A, Bladowska J, Neska M, Petryszyn K, Guziński M, Szewczyk P, et al. Quantitative MR evaluation of atrophy, as well as perfusion and diffusion alterations within hippocampi in patients with Alzheimer's disease and mild cognitive impairment. Med. Sci. Monit. 2013; 19: 86–94.

Zimny A, Szewczyk P, Trypka E, Wojtynska R, Noga L, Leszek J, et al. Multimodal imaging in diagnosis of Alzheimer's disease and amnestic mild cognitive impairment: value of magnetic resonance spectroscopy, perfusion, and diffusion tensor imaging of the posterior cingulate region. J. Alzheimers. Dis. 2011; 27: 591–601.

Zlokovic B V. Neurovascular mechanisms of Alzheimer's neurodegeneration. Trends Neurosci 2005; 28: 202–208.

Zlokovic B V. Neurovascular pathways to neurodegeneration in Alzheimer's disease and other disorders. Nat. Rev. Neurosci. 2011; 12: 723–738.

Zlokovic B V. Cerebrovascular effects of apolipoprotein E: implications for Alzheimer disease. JAMA Neurol. 2013; 70: 440–4.